# Thermal transients study for the ESS target helium cooling system

by Hannes Björk


LUND
UNIVERSITY

Thesis for the degree of Master of Science
Thesis advisors: Professor Jens Klingmann, Electrical & Instrumentation
Engineer Ola Ingemansson

To be presented, with the permission of the Faculty of Engineering of Lund University, for public criticism on the meeting at the Department of Energy Sciences on Thursday, the 9th of June 2022 at 09:00.

This degree project for the degree of Master of Science in Engineering has been conducted at the Division of Thermal Power Engineering, Department of Energy Sciences, Faculty of Engineering, Lund University.

Supervisor at the Division of Thermal Power Engineering was Professor Jens Klingmann. Supervisor at European Spallation Source was Electrical & Instrumentation Engineer Ola Ingemansson, assisted by Systems Engineer Per Nilsson.

Examiner at Lund University was Associate Professor Marcus Thern.

The project was carried out in cooperation with the Target division at the European Spallation Source.


Department of Energy Sciences
Faculty of Engineering
Lund University

ISSN: <0282-1990>
LUTMDN/TMHP-22/5502-SE

Typeset in LaTeX
Lund 2022

# Contents

# List of Figures

# List of Tables

# Nomenclature

**Symbols**

| | | |
|---|---|---|
| $c$ | Speed of sound | $[m/s]$ |
| $R$ | Molar gas constant | $[kgm^2/s^2Kmol]$ |
| $M$ | Molar mass | $[kg/mol]$ |
| $T$ | Temperature | $[^\circ C]$ |
| $\Delta T$ | Temperature difference | $[^\circ C]$ |
| $Q$ | Effect | $[W]$ |
| $c_p$ | Specific (isobaric) heat capacity | $[J/kgK]$ |
| $m$ | Mass | $[kg]$ |
| $h$ | Heat transfer coefficient | $[W/m^2K]$ |
| $d$ | Diameter | $[m]$ |
| $k$ | Thermal conductivity | $[W/K]$ |
| $\gamma$ | Heat capacity ratio | [1] |
| $j$ | Mass flux | $[kg/m^2s]$ |
| $\mu$ | Viscosity | $[Pas]$ |
| $A$ | Area | $[m^2]$ |
| $Q_m$ | Mass flow rate | $[kg/s]$ |
| $\alpha$ | Proportion | [1] |
| $P$ | Percent | [%] |

**Abbreviations**

*ESS* European Spallation Source

*LTH* Lunds Tekniska Högskola (Lunds University Faculty of Engineering)

*ETHEL* ESS Target Helium Experiments at LTH

*ARX* Auto Regressive model with exogenous input

*RTD* Resistance Temperature Detector

*NRMSE/D* Normalised Root-Mean-Square Error/Deviation

**Letter codes**

*YSV* Actuator operated shut-off valve

*F* Filter or separator

*V* Compressor, vacuum, pump, blower, or fan

*W* Heat exchanger

*TT* Transmitting temperature sensor

**Terms**

*Circulator* A fluid system component similar to a blower or compressor, but without a set pressure difference range.

*Primary cooling* The cooling system directly in contact with the heated object, i.e. the hottest cooling loop.

*Secondary cooling* The intermediate cooling loop, heated by the primary loop, and cooled by the tertiary loop.

*Tertiary cooling* The cooling system heated by the secondary or intermediate loop. Has no direct exchange with the primary loop.

*Krohne meter* An ultrasonic flowmeter of the Krohne brand.

# Sammanfattning

The European Spallation Source (sv: Europeiska Spallationskällan) kommer att bli den mest kraftfulla spallationskällan i världen när den är i drift vid full kapacitet. Neutronerna som används av vetenskapsmän och ingenjörer är spallerade från ett roterande hjul av volfram, som blir bombarderat av accellererade protoner. Hjulet, även kallat målet, upplever värmeutveckling under spallationsprocessen, och är därför kyld av ett kylningssystem som använder helium. Målets primära kylsystem, även kallat system 1010, har blivit modellerat i programmeringsspråket Modelica, men är varken fullt verifierad eller praktiskt utvärderad.

ETHEL är en test-rigg placerad vid LTH, och liknar system 1010 i funktion. Den kan användas för att utföra experiment, och resultaten kan till viss grad extrapoleras till system 1010. En modell av ETHEL var konstruerad. Modellen hade syftet att vara både trogen till de fysikaliska begränsningarna för ETHEL, och att konstrueras lika nog system 1010 modellen för att kunna extrapolera gjorda slutsatser.

Transienta experiment formulerades, baserade på förväntade funktionsavbrott för system 1010. Experimenten utfördes på ETHEL-riggen, ETHEL-modellen, samt system 1010 modellen. Baserat på resultaten från experimenten utvärderades ETHEL modellen, både i avseende på tidssvar, samt avseende på dataavvikelse.

Systemidentifiering på både system 1010 modelldatan och datan från ETHEL utfördes, med syftet att bedöma betydelsen av sensor-placering med den förstnämnda datan, samt att bedöma den relativa snabbheten med den sistnämnda. Tre sensortyper undersöktes i avseende av snabbhet, men analysen saknade verktygen att avgöra sensorns pricksäkerhet. Placeringsanalysen visade att sensors placering i system 1010 modellen inte signifikant påverkade tidssvaret.

Modellutvärderingen visade att ETHEL-modellen presterad kvalitativt bra, den visade tidssvar som väl jämfördes med det riktiga datan, men att betydande kvantitativa fel upptäcktes. Resultaten extrapolerades till system 1010 modellen och dess riktiga motsvarighet. Resultaten implicerade att placerings-analysen var trogen till det riktiga system, och vidare slutsatser kring detta resultat kunde dras.

# Abstract

The European Spallation Source (ESS) is going to be the worlds most powerful spallation source once in full operation. The neutrons used by scientists and engineers are spallated from a rotating wheel of wolfram, being bombarded by accellerated protons. The wheel, also called the target, develops heat in the process, and is therefore cooled by a helium cooling system. The target primary cooling system, named system 1010, is modelled in the language Modelica but is not fully verified, nor has any practical testing been conducted.

ETHEL is a test rig located at LTH, similar in function to that of system 1010. It can be used to conduct experiments, and the results can to some degree be extrapolated to system 1010. A model of ETHEL was constructed. The model was intended to both be faithful to the physical contraints of ETHEL, but also constructed similarly enough to the system 1010 model to allow for extrapolation of the conclusions made.

Transient experiments were formulated, based on expected cases of failure for system 1010. The experiments were conducted on the ETHEL rig, the ETHEL model, and the system 1010 model. Based on the experiment results a model evaluation of the ETHEL model was conducted, both in regards to time-response behaviour, and in regard to data error.

System identification on both the system 1010 model data, and the ETHEL data was conducted, with the purpose to identify significance of sensor location in the former case, and to determine the relative speed of the sensors in the latter case. Three sensor types were examined for their speed, however the analysis lacked the tools to evaluate their accuracy. The location analysis revealed that the exact location of the sensor in the system 1010 model did not significantly impact the time-response.

The model evaluation showed that the ETHEL model performance was qualitatively good, demonstrating a good time-response compare to the real system, however significant quantitative errors were found. The results were extrapolated to the system 1010 model and its real counterpart. This implies that the location analysis is fair to the real system, and further conclusions about this fact was made.

# Chapter 1.

# Introduction

## 1.1. Background

### 1.1.1. European Spallation Source

The European Spallation Source (ESS) is a neutron source under construction that can be used by scientists for research within the fields of materials and life sciences, energy, environmental technology, cultural heritage and fundamental physics [1]. The construction of one of the largest science and technology infrastructure projects being built today began in 2014, and is deemed to be completed in 2027, with the covid-19 pandemic being cited as one of the major reasons for delays [2, 3]. An overview of the ESS facility, the exterior of which fully built can be viewed in figure 1.1.

ESS is organised under the European Research Infrastructure Consortium's (ERIC) legal framework, and the ESS council is the highest governing body of the facility [4]. In the consortium there are 13 founding countries, and the project is reliant on the European expertise that the cooperation brings [4].

The neutron source allows scientists and engineers to study the dynamics of atoms and molecules over a large span of space and time, "from micrometres to one-hundred-thousandth of a micrometre, and from milliseconds to ten-million-millionths of a millisecond", according to the ESS promotional material [6]. Neutrons are used to great effect to study the behaviour of individual atoms and molecules [7]. Neutrons allow us to probe structures on very small length scales, and the wave-like nature of the neutron causes them to produce interference patterns, which can be used to understand crystal structures [8]. Furthermore, neutrons are able to gain or lose energy as they interact with materials, giving us more information about the material [8].

**Figure 1.1.:** Birds-eye view of the ESS facility. Photo: Perry Nordeng/ESS [5].

### 1.1.2. Helium cooling system

The tungsten target and the supporting steel structure, that get struck by the accelerated protons are cooled by helium gas, circulating in a closed loop. This cooling system is called the target primary cooling system, or system 1010, and makes up a major part of the target cooling system along with other subsystems and supporting systems [9].

Cooling is necessary to prevent hot spots and local melting in the wolfram, caused by the large amount of heat deposited from the proton beam [10].

### 1.1.3. Modelling and Modelica

Cooling of the tungsten target is as explained critical to safe and continuous operation of the ESS plant. Therefore, control of the cooling system is necessary to keep temperatures in the target at a desired level. The foundation of any control design depends on having a model of the process that one is trying to control [11].

The Modelica Language is a programming language used for modelling complex systems such as mechanical, thermal, or electrical systems. The Modelica library furthermore provides the user with some base-level components used for modelling [12]. ESS uses the Modelica Language for modeling of their systems [13].

ESS has constructed a model for the target primary cooling system which is only partially validated [13]. However there is still a need for practical tests for events that can cause thermal transients, and to practically evaluate the model.

### 1.1.4. Systems, transients and sensors

In his 2011 book Karel J. Keesman describes modelling as follows: "a critical step in the application of system theory to a real process is to find a mathematical model which adequately describes the physical situation" [14]. Furthermore mathematical system identification is a tool to estimate good models of systems. The term "good" means useful in our application of the model.

Most often, the procedure of system identification and model verification includes a design of appropriate experiments, based on prior knowledge of the system and the objectives of the modelling at hand. The data collected can in turn be used to evaluate the proposed model [14].

Sensors are a critical point of a system if it is to be controlled, as they could introduce delays or other disturbances in the system if not compensated for. It is therefore desired to evaluate the use of sensors in system 1010, both different types of sensors and the placement of sensors, both in regard of their time response and their accuracy.

## 1.2. Main goals

- Model ETHEL in the same regard as how the system 1010 model was constructed.
- Formulate expected cases that generates thermal transients in system 1010.
- Perform experiments meant to emulate the transient cases for ETHEL, the ETHEL model, and the system 1010 model.
- Empirically evaluate the ETHEL model, with data from the experiments, and extrapolate to the system 1010 model.
- Analyse sensors, based on the experiments, especially in regard to sensor type and location.
- Propose changes to, or areas of further research on, the system 1010 model, and system 1010 itself.

## 1.3. Delimitations

In this paper the systems mentioned are assumed to be in operation as expected, and no abnormal or accident scenarios are accounted for. These cases are left for the associated risk and hazard analyses.

While investigating transients only expected initiators will be considered, i.e. events that are supposed to happen. Examples for these events can be compressor shutdown, or primary side of a heat exchanger stopping. This does not include for example a piping rupture, a heat exchanger puncture, or other unexpected failures.

# Chapter 2.

# Theory

## 2.1. Modellica and simulation

The Modelica language is a language designed for modeling of systems, by means of acausal connections between components. The connections are described as mathematical equations, and are solved by an iterative solver. Modlica is object-oriented, meaning that components can be reused, and the models are user-friendly [15].

The package Modelica, or the Modelica Standard Library, is a library containing standard components and interfaces from multiple engineering disciplines, one of which is the Modelica Fluid library [16]. The Modelica Fluid library provides components for thermo-hydraulic systems, the purpose of which is, among others, to provide standard connectors and a reasonable set of components for use in thermo-hydraulic process modelling [17]. The fluid librarys connectors are designed in order to ensure that mass and energy balances are fulfilled at any given connection point but also to preserve momentum balance, overall [17].

A common issue within the topic of fluid simulation is the zero-flow problem. When a flow is close to zero the flow is seen as sporadic and the step solver takes smaller and smaller steps to find a solution. Therefore the computation times increase drastically [18]. This implies that close to zero-flow simulations are impractical and should be avoided.

## 2.2. Model evaluation

There are many schools of thought when evaluating a model in contrast to actual test data. One method is to calculate the NRMSD, or the NRMSE, between the model output and the real output. This is the method used in MatLab System Identification toolbox [19]. The NRMSD is calculated in equation 2.1, where $N$ is the total number of data

points, $y$ is the reference data, and $\hat{y}$ is the test data [20].

$$\begin{aligned} \text{RMSD} &= \sqrt{\frac{\sum_i^N (y_i - \hat{y}_i)^2}{N}} \\ \text{NRMSD} &= \frac{\text{RMSD}}{y_{max} - y_{min}} \end{aligned} \tag{2.1}$$

A more readable figure can be obtained in equation 2.2, where a percentage of fit, of sorts, can be calculated [21].

$$P_{fit} = (1 - \text{NRMSD}) \cdot 100 \tag{2.2}$$

Relative error is a measure of numerical precision in a general sense, and is easily extrapolated to other cases. The relative error at sample $i$ is given by equation 2.3, where $y$ is the reference data and $\hat{y}$ is the test data [22].

$$e_i = \frac{|\hat{y}_i - y_i|}{y_i} \tag{2.3}$$

A way to estimate the accuracy of two data sets in a temporal perspective is to examine the cross-correlation, and the correlation coefficient of the data sets. In the case of model evaluation the data sets to be examined is the output of the model and the output of the real system, given the same input. The cross-correlation provide a measure of association between signals. The data sets can be normalised for the mean of the data sets, as well as the cross-correlation normalised over the root auto-correlation for both data sets. In equation 2.4 the full calculation is done, where $x$ is one data set, $y$ is the other data set. $\bar{x}$ and $\bar{y}$ is their respective means. The cross-correlation $\rho$ is dependant on an input lag $l$ [23].

$$\rho(l) = \frac{\sum_i (x_i - \bar{x})(y_{i-l} - \bar{y})}{\sqrt{\sum_i (x_i - \bar{x})}\sqrt{\sum_i (y_i - \bar{y})}} \tag{2.4}$$

The correlation coefficient, meaning Pearsons product-moment correlation, can be derived from fitting a straight line to a scatterplot made out of the normalised data sets, each point being a two-dimensional coordinate made from the output from the model and the output from the real data, at a certain time. The angle of the straight line is thus the correlation coefficient [23]. A correlation coefficient over 0.8 is considered a strong

positive correlation [24].

## 2.3. Speed of sound and estimation of fluid mixture

An ultrasonic flowmeter effectively measures the speed of sound in a medium [25]. When placed close to a traditional temperature sensor conclusions can be made about the contents of the fluid. In some cases it may be useful to estimate the proportions of two fluids in a mixture, for instance helium and air.

In an ideal gas the speed of sound $c$ is described in equation 2.5, where $\gamma$ is the adiabatic index, $R$ is the molar gas constant, $M$ is the molar mass of the fluid, and $T$ is the temperature of the fluid [26].

$$c = \sqrt{\frac{\gamma \cdot R \cdot T}{M}} \tag{2.5}$$

A fluid mixture, made up of two fluids, has a molar mass that is an average of the mass fractions contributed by both fluids. In equation 2.6 the average molar mass of a helium and air mixture is calculated, where $\alpha$ is the proportion of air.

$$\frac{1}{\bar{M}} = \alpha \cdot \frac{1}{M_{air}} + (1 - \alpha) \cdot \frac{1}{M_{he}} \tag{2.6}$$

If $\bar{M}$ was to be perfectly calculated, $\alpha$ could be derived, however, uncertainties in the physical properties of the fluid mixture leads to the calculation to be flawed, as the adiabatic index for the fluid mixture is not known. Most importantly, if the adiabetic index was to be estimated, for example a value between the two fluid components, the limits of $\alpha$ would be skewed. For example if the fluid mixture contained 100 % air, but the adiabetic index would be estimated to 1.5, $alpha$ would never be 1, even under ideal conditions.

Another method could be to compare the speed of sound in both fluid components, to the measured speed of sound. The method would lead to errors between the limits of $\alpha$, as the linear average molar mass depends non-linearly on the speed of light, but it would preserve the limits, i.e. 100 % air in the fluid mixture would give an $\alpha$ of 1 under ideal conditions. This is the method used in this paper.

The method described is portrayed in equation 2.7, where $\alpha$ is the proportion of air in

the fluid mixture, $c_{he}$ is the speed of sound in helium for the given temperature, and $c_{air}$ is the speed of sound in air for the given temperature.

$$\alpha = \frac{c_{\text{measured}} - c_{he}}{c_{air} - c_{he}} \tag{2.7}$$

## 2.4. Heat transfer

The general equation for heat transfer to a system of weight $m$, specific heat capacity $c_p$, and temperature difference $\Delta T$ is given in equation 2.8 [27].

$$Q = m \cdot c_p \cdot \Delta T \tag{2.8}$$

The heat capacity, $C$, of a system is given by equation 2.9 where $c_p$ is the specific heat capacity, and $m$ is the mass [27].

$$C = c_p \cdot m \tag{2.9}$$

The heat transfer coefficient for a given pipe section is related to the heat transfer coefficient of the layers of the pipe (insulation, pipe material), the medium in the pipe, and the medium outside the pipe as in equation 2.10 [27, 28].

$$\frac{1}{h} = \frac{1}{h_{\text{inner medium}}} + \frac{1}{h_{\text{insulation}}} + \frac{1}{h_{\text{pipe material}}} + \frac{1}{h_{\text{outer medium}}} \tag{2.10}$$

Each heat capacity for a given layer in a given pipe section is given by equation 2.11, where $k$ is the thermal conductivity of the layer material, $d_i$ is the inner diameter of the layer, and $d_o$ is the outer diameter of the layer [28].

$$h = \frac{2 \cdot k}{d_i \cdot \log\left(\frac{d_o}{d_i}\right)} \tag{2.11}$$

According to the Dittus-Bölter correlation, for fluid flowing in a pipe the heat transfer from the medium to the pipe can be expressed as equation 2.12, where $k$ is the thermal conductivity of the fluid, $d$ is the hydraulic diameter, $\mu$ is the fluid viscosity, $j$ is the mass flux, $c_p$ is the isobaric heat capacity for the fluid, $n$ is 0.4 if the pipe is heating the fluid, and 0.33 if the fluid is heating the pipe. The conditions are that there is no boiling, condensation, nor significant radiation from the fluid [29].

$$h = \frac{k}{d} \cdot 0.023 \cdot \left(\frac{j \cdot d}{\mu}\right)^{0.8} \cdot \left(\frac{\mu \cdot c_p}{k}\right)^{n} \tag{2.12}$$

| | Air | Helium | Steel | At temperature |
|---|---|---|---|---|
| $k\ (W/mK)$ | 0.0333 [31] | 0.1906 [31] | 45 [32] | 126.85 °C |
| $\mu\ (10^{-5}Pa \cdot s)$ | 2.2 [33] | 2.32 [33] | - | 100 °C |
| $c_p\ (10^3 J/kgK)$ | 1.01 [34] | 5.19 [34] | - | - |

**Table 2.1.:** Material and medium parameters.

Furthermore the mass flux, $j$ is described by equation 2.13, where $Q_m$ is the mass flow rate and $A$ is the cross sectional area orthogonal to the flow direction [30].

$$j = \frac{Q_m}{A} \tag{2.13}$$

Some of the parameters that are properties of mediums or materials are presented in table 2.1.

## 2.5. System identification

System identification is a broad field with many applications. In this project, however, it is used to evaluate system outputs and data from a perspective of "speed", i.e. time to convergence and time to response, as a separate variable from the amplitude or gain of outputs and data. It is a useful comparison when making conclusions of the qualitative and quantitative quality of models and other systems.

Delay estimation, or dead-time estimation, is part of system identification. One method to estimate a delay between an input signal and an output signal is to minimise the error of an estimated ARX model over variable delays. This method is described in equation 2.14, where $n_a$ is the order of the ARX model disturbance polynomial, $n_b$ is the order of the ARX model input polynomial, and $d$ is the delay. $u(t)$, $y(t)$, and $e(t)$ are the input, output and disturbances respectively [35].

$$y(t)+a_1y(t-1)+...+a_{n_a}y(t-n_a) = b_1u(t-d)+...+b_{n_b}u(t-n_b-d+1)+e(t) \tag{2.14}$$

One model that can be used for system identification is transfer functions, i.e. a polynomial in the frequency plane, in a general form seen in equation 2.15. The transfer function for a system can be estimated with a given set of zeroes, $n_b$ (order of polynomial $B(q)$), and poles, $n_f$ (order of polynomial $F(q)$). The error for variable parameters $b_i$ and $f_j$ is minimised compared to the given output data, as seen in equation 2.16. Furthermore, in some cases it is useful to assume the system has one pole and no zeroes,

when comparing the time-dependant behaviour of the system [36].

$$y(t) = \frac{B(q)}{F(q)}u(t-d) + e(t) \tag{2.15}$$

$$B(q) = b_1 + b_2 q^{-1} + ... + b_{n_b} q^{-n_b} + 1F(q) = 1 + f_1^{-1} + ... + f_{n_f} q^{-n_f} \tag{2.16}$$

The poles in a single pole transfer function effectively show how "fast" or "slow" a system is. In general terms a system has a more rapid ascent or descent to its steady state value the further away the pole is from the imaginary axis, assuming that the pole is real and negative. It may therefore be a useful descriptor when analysing the "speed" of systems, meaning how fast a system settles [37].

# Chapter 3.

# System descriptions

## 3.1. System 1010

The target helium cooling system broadly consists of four subsystems: the target primary cooling system (system 1010), the pressure control and helium storage system (system 1011), the helium injection system (system 1013) and the helium purification system (system 1015) [38]. In total the loop encloses 11.7 $m^3$ and is expected to be filled with 15 kg of helium [9].

As an overview, the target primary cooling system (system 1010) consists of three tube and shell heat exchangers, two compressors, two filters, one optional filter and the target wheel [39]. A simplified version of this system can be seen in the diagram in figure 3.1. Note that the target bypass line is controlled by an unnamed valve, used only for testing, and not explored further.

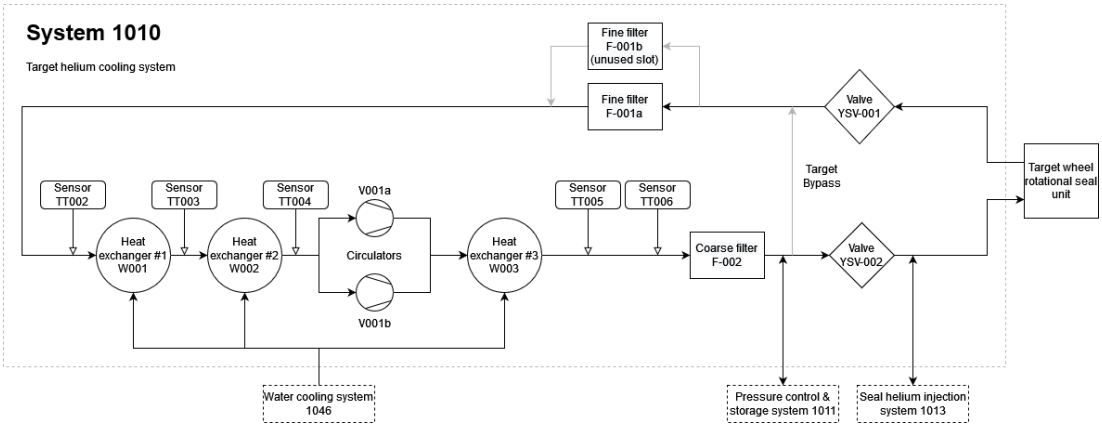


**Figure 3.1.:** Simplified diagram of the Target Helium Cooling system.

### 3.1.1. System delimitations

Some peripheral systems of the target helium cooling system are not included in figure 3.1: the helium purification system (system 1015), monolith rough vacuum pump system (system 1027), helium seal injection system (system 1013), and decontainment solution (system 1049) [39]. As explained further, these subsystems have little to no impact on the thermal behaviour of the target cooling system.

The monolith rough vacuum pump system is used to keep the monolith at a rough vacuum ($\leq$ 100 Pa) during operation, and assuming non-faulty operation it should not impact the primary target cooling to any discernible degree [40].

The de-containment solution is a drain system for contaminated materials that is not relevant to the thermal behaviour of the target helium cooling system [39].

As stated by the relevant technical specifications the throughput of helium through the helium purification system is 1.5 - 3.0 g/s, while the flow rate as the point of diversion is 1500 - 2850 g/s. The diverted flow is very minor (0.1%), in comparison to the normal flow, and the thermal impact of this system can safely be ignored [41].

Furthermore, the helium seal injection system is also a non-direct part of the cooling function, and the helium flow through the system is extremely low assuming the rotary seal on the monolith is working properly [9].

### 3.1.2. Pressure control and helium storage system

The function of the pressure control and helium storage system during operation is to keep the helium pressure in system 1010 as close to a set point as possible. The system employs a pressure controller that controls a valve to a chamber of helium nominally pressurised to 1 bar or less. Furthermore the system contains a storage system for excess helium when the pressure in system 1010 is decreasing [9].

The most common action for the pressure control and helium storage system during operation, however, is to replenish leaked helium from system 1010 [9].

### 3.1.3. Piping

The cold side of system 1010, i.e. the section downstream of the first heat exchanger up until the target uses DN200 pipes, with an inner diameter of 206,1mm. Meanwhile the the warm side of the system, i.e. the section downstream of the target up until the first heat exchanger, is built with DN250 pipes, with an inner diameter of about 263mm. The DN200 pipes add up to a total length of 48.2 m, and the DN250 pipes add up to a total length of 48.1 m [9]. Furthermore the pipes are planned to be covered with 80 mm of insulation to decrease heat losses to the environment [13].

### 3.1.4. Heat exchangers

The system 1010 heat exchangers, W001, W002, and W003 are all tube-and-shell heat exchangers enclosing 0.79m$^3$, 1.16m$^3$, and 1.05m$^3$ of helium respectively, and whereof the first heat exchanger is co-flow and the remaining two are counter-flow [9]. The heat exchangers use water on the secondary side, connected to system 1046, with the inlet water temperatures 55 °C, 30 °C and 30 °C for W001, W002, and W003 respectively [9, 39].

### 3.1.5. Circulators

The system 1010 cooling loop contains two circulators running in parallel. The use of the term circulators to describe the machines was employed to avoid confusion over the function of the machines. Such a term is used instead of terms compressor, fans, or blower, that imply a specific range of pressure difference over the machines.

The circulators are of a high speed variation, and spin up to 40000 rpm to force the helium around the cooling loop [42]. The helium flow for cooling the maximum 5 MW of heat deposited in the target is 2.7 kg/s [9]. Therefore each of the circulators is designed for a mass flow of 1.425 kg/s [43]. Each of the circulators is expected to increase the pressure by 143.1 kPa, but the designed pressure increase over both circulators is 130 kPa [39, 43].

### 3.1.6. Filters

The cooling circuit contains two filters, one being a coarse filter ($> 5\ \mu$m), and the other being a range of fine filter slots ($> 0.05\ \mu$m), where only one slot is intended to be used at installation.

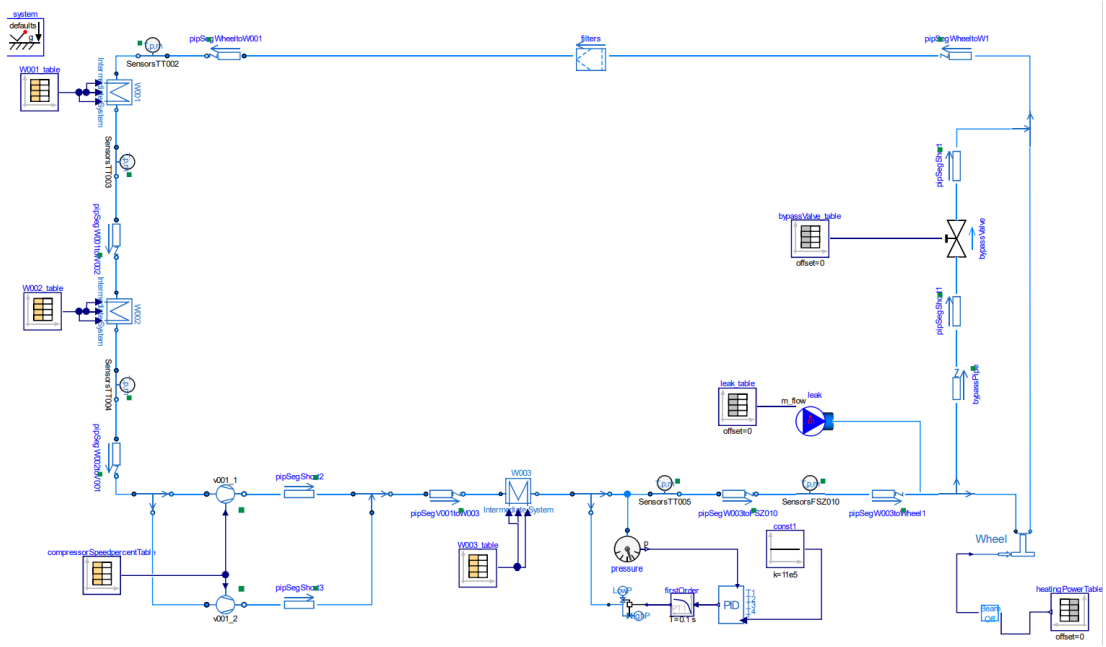


**Figure 3.2.:** Overview of the system 1010 model.

## 3.2. System 1010 model

A model of system 1010, presented in figure 3.2, was previously built in Modelica primarily using Modelicas standard fluid and thermal libraries [13].

### 3.2.1. Pipes and filters

The piping in the system 1010 model was effectively implemented in two parts: heat capacity of the pipe material and convection from the pipe to atmosphere, where the temperature is assumed to be a constant 20 °C. The pipe segment model is graphically represented in figure 3.3

The fine filter section is represented as reconfigured pipes with a slightly different size and much higher flow resistance (ca. 500 times higher). The rough filter is not included in the model.

### 3.2.2. Heat exchangers

As the Modelica standard libraries do not contain a sufficiently detailed heat exchanger model, the models for the system 1010 heat exchangers were built individually [44]. The

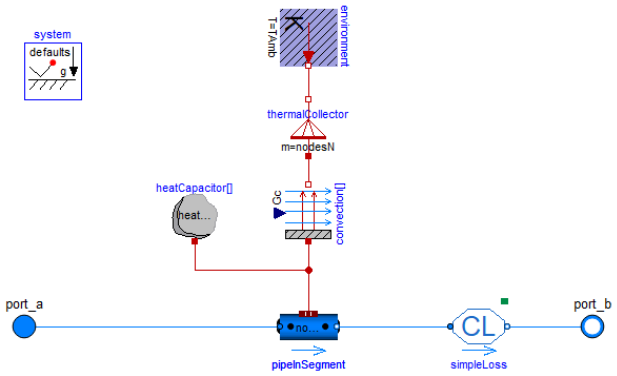


**Figure 3.3.:** Model of pipe segment used in system 1010 and ETHEL.

decision was therefore made to employ Modelica standard library DynamicPipes but write a custom heat transfer function. These pipes are also connected to a heat capacity, through a conduction block, as to emulate the mass of the pipes.

This structure is used at two points, between the primary and secondary system, and between the secondary and tertiary system. The primary side being helium flowing through system 1010, the secondary side being a closed loop of water between the two other systems, and the tertiary system being a constant flow of water of a constant temperature.

The secondary side of the heat exchanger flows in either the same direction as the primary side, a co-flow heat exchanger, or against the direction in the primary system, a counter-flow heat exchanger. W001 being a co-flow heat exchanger, and W002 and W003 both being counter-flow heat exchangers.

The secondary side in the heat exchanger is a closed loop, and employs a small volume, and a controlled pump, controlled around the mass flow, to circulate the water.

The tertiary system is a water source and water sink of constant temperature and flow rate.

The water flows in the secondary systems are 7.14 kg/s, 5.4 kg/s and 5.7 kg/s for W001, W002, and W003 respectively. The tetriary systems has a flow of 6 kg/s in all cases, furthermore have a temperature of 49.85 °C, 24.85 °C, and 24.85 °C for W001, W002 and W003 respectively.

### 3.2.3. Circulators

The system 1010 circulators are modelled as simple Modelica standard fluid library prescribed pumps, configured with the volume flow rate and pressure head given from the circulator technical specifications.

### 3.2.4. Target wheel

The target wheel is modelled as a series of heat capacities, connected to a standard library DynamicPipe, in this section this singular structure is referred to as a block. There are a total of 8 of these blocks, the helium flows from block 1 to block 8. They are then interconnected by a heat conductor in an overlapping manor, i.e. block 1 is connected block 8, block 2 is connected to block 7, block 3 is connected to block 6 and block 4 is connected to block 5.

In block 5 and block 6 the heat effect is applied, obtained from the component input.

Furthermore, a separate closed circuit is created. This consists of a helium source and sink using the measured temperature and pressure from the main loop. The heat is applied in this section as well, as is heat flow through a heat conduction component from the main target wheel loop. A heat capacity is also connected to this section. The purpose of this fully separated loop to investigate the temperature of the hottest part of the helium in the target wheel.

### 3.2.5. Pressure control and helium storage system

A pressure control system is implemented in the system 1010 model loop. The main purpose of this system, as previously stated, is to remove helium through a compressor, and to add helium from a high pressure container, as to keep a constant pressure in system 1010.

The pressure is measured and controlled by to a PID-controller. The PID-controller is compared to the nominal pressure times the mean momentary temperature divided by the nominal temperature in the system at the nominal pressure. The controller signal is fed through a low-pass filter to the component conducting the actuation upon the helium in the main circuit.

In this component the control signal is divided into the high actuation, leading helium from a high pressure (2000 kPa) helium source, and a low actuation, a subsystem

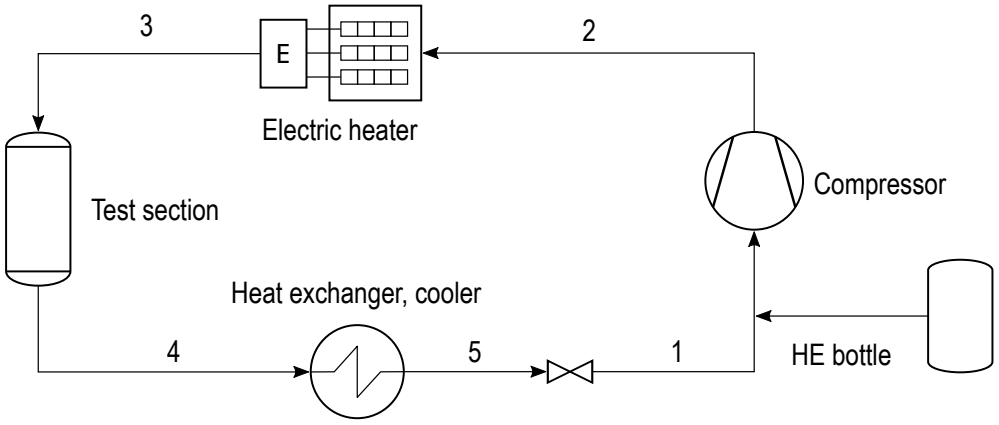


**Figure 3.4.:** Simplified diagram of ETHEL, the test rig.

composed of a compressor, volume, and a basic heat exchanger, forcing away helium from system 1010. Along with this main function the component also includes a safety system preventing zero compressor flow, which would induce long computing times.

The nominal pressure and temperature controlled around in the model is 1100 Pa and 60 °C respectively.

### 3.2.6. Leakage

A simple leakage is included in the model as a helium sink. The leakage amount is predefined as 0.0005 g/s, or $5 \cdot 10^{-7}$ kg/s.

## 3.3. ETHEL

ETHEL is a helium circulation system at LTH, originally used to investigate various aspects of cooling tungsten with pressurised helium [45]. The ETHEL loop contains a booster compressor, an electric heater, a test vessel, and a cooling heat exchanger, with water on the secondary side. The loop also contains a pressure maintaining valve and a flow meter, the latter being located in position 2 in figure 3.4. In a later stage four temperature sensors of type TC and one of type RTD were installed, along with an ultrasonic flowmeter [46, 47]. The system is depicted in figure 3.4. Five sensors are placed in a position according to figure 3.5, where $T_{\text{heater}}$ is only used for internal heat control and the data from it cannot be recorded. One thermocouple sensor is placed in position 5, and a pressure sensor is placed by the test section in position 3, see figure 3.4.

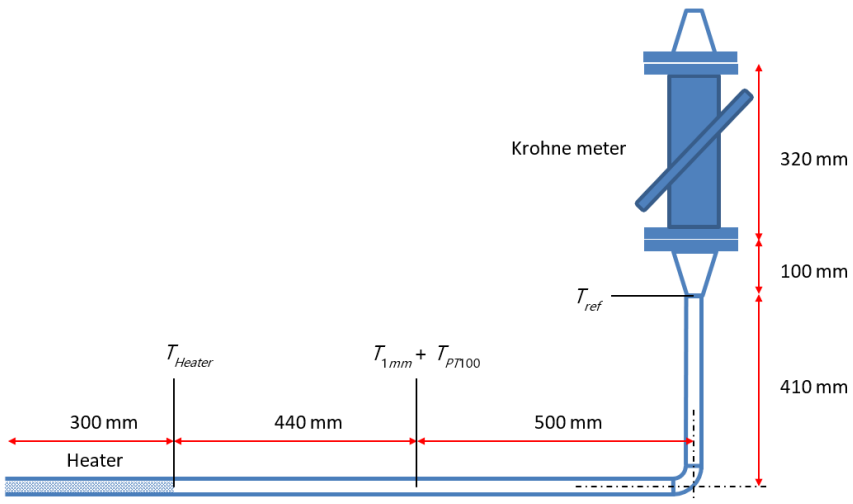


**Figure 3.5.:** Ethel lab setup. Section with heater, temperature sensors, and ultrasonic flowmeter [47].

See more images of ETHEL in appendix A.

# Chapter 4.

# Modelling ETHEL

The model of ETHEL was mainly implemented using Modelica standard library components, as is the system 1010 model. Broadly, the system contains four parts: the heat exchanger, the electric heater, the pump & control valve, and the piping & the test section.

The final model is presented in figure 4.1.

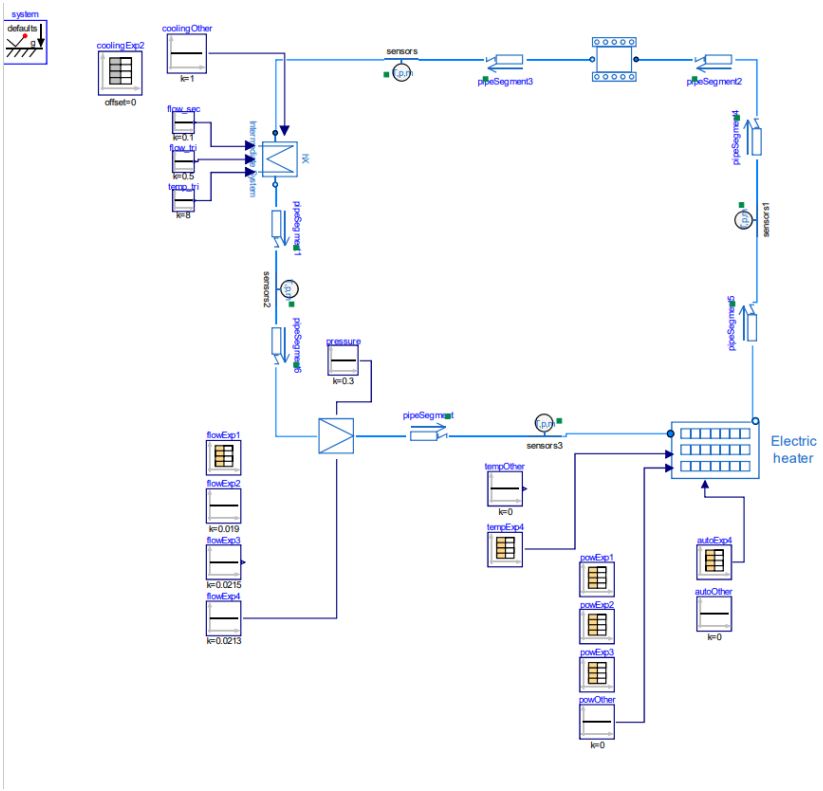


**Figure 4.1.:** Overview of the ETHEL model.

## 4.1. Heat exchanger

The heat exchanger in the ETHEL model is essentially derived from three circuits: the primary circuit of helium, the secondary closed circuit of water, and the tertiary circuit of a set temperature water.

The primary and the secondary models transfer heat through a thermal conduction block, connected to a volume the size of the real ETHEL heat exchanger. From measurements it is determined that the ETHEL heat exchanger is cylindrical, with a length of 1m and a radius of 77 mm. Measuring the radius of the inner pipe to 10.5 mm and assuming it makes 3 passes through the outer cylinder gives the estimation of 0.01783 $m^3$ total water volume in the heat exchanger.

Furthermore, the secondary circuit is required to have the ability to reduce the flow rate to zero, as to allow for certain experiments. However, because of the zero-flow problem simply turning off the flow rate on the secondary circuit would be impractical. A bypass pipe and boolean valves were therefore implemented, to allow for total flow stop through the volume.

It is also known that the normal flow through the secondary system is 0.4 $m^3$/h, or 0.11 kg/s, as read off the installed pump. The flow is implemented in the model with a fluid sink and a fluid source, which maintains the fluid temperature.

The tertiary system has a set temperature of 8 °C, and an unknown flow rate. The secondary circuit transfers heat through a thermal conduction, using Modelica standard library DynamicPipes. Again, the tertiary system is created by a sink and a source of given temperature.

An image of the component model can be seen in figure 4.2.

## 4.2. Compressor and control valve

Information and documentation on the ETHEL compressor were lacking: furthermore the exact setting and function of the control valve were not recorded. Therefore, it was decided that the compressor and the control valve would be modelled as a controlled compressor and a linear valve.

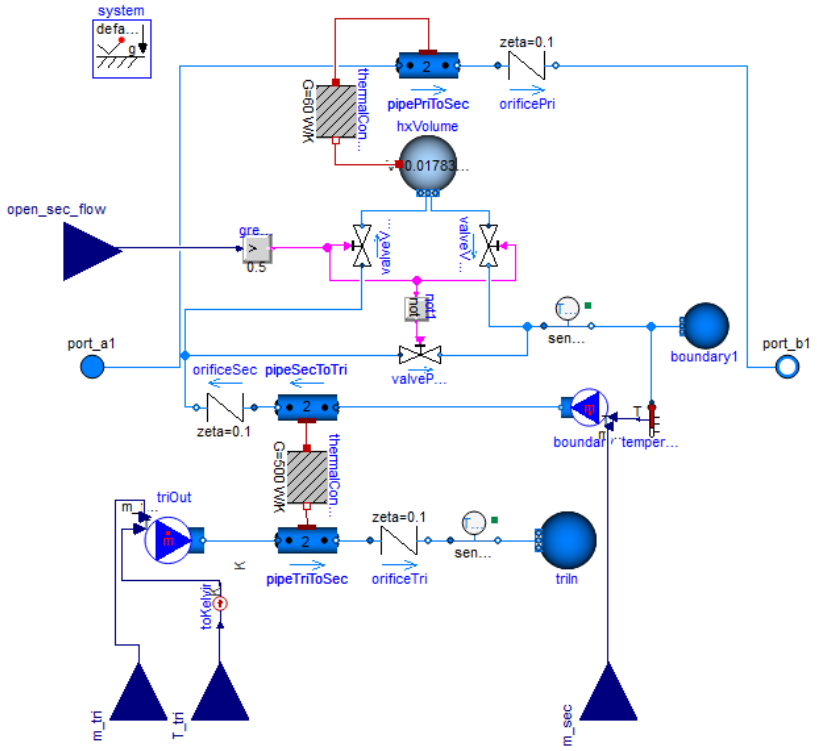


**Figure 4.2.:** Model of heat exchanger used in ETHEL.

The controlled compressor controls to a given mass flow rate, implying that the mass flow rate is used as an input. The linear valve was adjusted to increase pressure to an appropriate level (around 700 kPa).

Some caution must therefore be taken when analysing the pressure and mass flow rate results from the ETHEL model simulation, where the former is estimated to a range, and the latter is used as an input from the real experiment.

## 4.3. Piping and test section

The piping in the ETHEL model is modelled functionally the same as the piping in the system 1010 model, see figure 3.3, however readjusted for the size, and recalculated for the convection of the real ETHEL pipes.

The size of the model pipes was adjusted to the real size of the pipes. The average pipe outer diameter of ETHEL was measured to 32mm, and the inner diameter is estimated to be 30mm.

The parameters of the Modelica convection object is adjusted for the thermal conductance of the pipe, which in turn is a product of the heat transfer coefficient and the area of conductance, the former being calculated from equations 2.10, 2.12, and 2.11.

Furthermore we calculate the heat capacity of the pipe material from equation 2.9, and the measured inner and outer radius.

Almost all piping in ETHEL is uninsulated, however, the pipe segment directly upstream from the test section is a short pipe section with insulation. The heat transfer coefficient for this section was calculated as before, but including insulation.

The test section is implemented as a pipe with adjusted parameters, the width is estimated as an average and calculations were done as before. Effectively it is modelled as a much thicker pipe.

## 4.4. Electric heater

The ETHEL loop contains a simple electric heater, driven by a controller. The controller can be put into an automatic mode, where the applied effect from the heater is dependent on the measured temperature from a thermocouple directly downstream of the heater (seen in appendix A), controlled by using simple PID control. Alternatively, the controller can be put into a manual mode, where it outputs a constant percentage of the total power output of the electric heater. Both these features would need to be captured in the model, as both features will be used.

Furthermore, the electric heater in ETHEL can be turned off by flipping a switch, creating a break in the controller output signal. This, however, does not stop the controller action and leads to an integrator windup. For longer durations of off time the controller will always give out 100% power when initialised, leading to overshoots.

To capture these properties in the electric heater model, a standard library PID controller is connected to a switch, allowing to model switching between power set-point and temperature set-point during runtime. The heat is applied through Modelicas standard library DynamicPipe. The measurements for the PID control are taken after a pipe segment, downstream of the heated pipe.

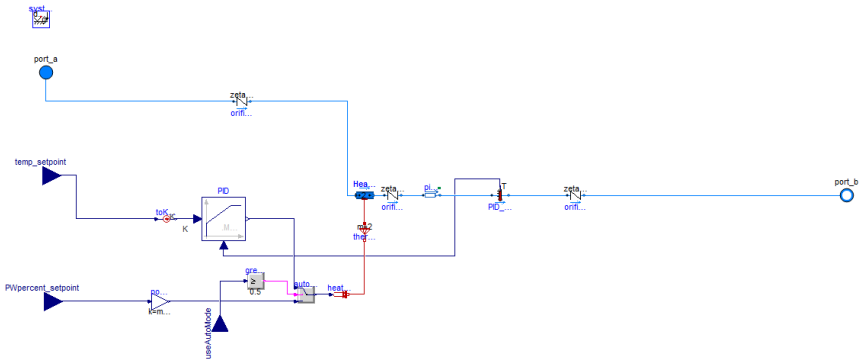


**Figure 4.3.:** Model of electric heater used in ETHEL.

In figure 4.3 the model of the electric heater is depicted graphically in Modelica.

# Chapter 5.

# Transient experiments

## 5.1. Deriving transient experiments

Analysis of the transients will take some expected cases into account.

In a qualitative radiological hazard analysis a decreased cooling efficiency upon the target wheel and the consequences thereof are investigated. Some of the cited initiators during operation directly related to the target primary cooling system are, circulators that fully or partially stop, leading to a decreased helium flow through the cooling loop [10]. The decrease in flow can also be caused by the filters or pipes getting clogged, according to the report [10]. The ETHEL test rig is limited in the amount of change in flow one can do during operation. However, by decreasing the pressure on the low-pressure side of the compressor, one will effectively decrease the mass flow in the loop. This case will be referred to as experiment 1.

A loss in the intermediate cooling water flow, being the water flow in system 1046, is also named as an initiator of loosing cooling efficiency [10]. In ETHEL this can be accurately represented by turning off the intermediate coolant pump in the secondary cooling circuit. This case will be referred to as experiment 2.

A scenario where the proton beam power exceeds the maximum design value is also considered, meaning that the deposited heat in the target wheel may be higher than expected, or otherwise sporadic. The initiator is cited as controls failure in the accelerator [10]. To emulate this for the ETHEL system a simple step of the power of the electric heater can be used, and will enact an increase of the supplied power to the cooling loop. This will be referred to as experiment 3.

Furthermore it is of interest to investigate the step response of the sensors, to investigate the sensor models and the time delay of the sensors. The purpose is to lead to conclusions

that will improve the control of system 1010, regarding the sensors. This case will be referred to as experiment 4.

## 5.2. Experiment 1: Decreased helium flow in system 1010

### 5.2.1. ETHEL and ETHEL model

To emulate the decrease in the mass flow in the ETHEL system we decrease the pressure on the low-pressure side of the compressor using the control valve, ideally from the highest pressure possible (500 kPa) to the lowest pressure possible (350 kPa). This will give the largest step down possible for the mass flow through the loop. The manoeuvre will be executed during normal operation with the active heating and cooling elements. Furthermore, the heater will be set to a manual mode, where the user controls the amount of power supplied to the system up to 5 kW.

1. The system runs as normal at maximum pressure. ( 500 kPa on low pressure side, 1000 kPa on high pressure side) Data from relevant sensors are captured.
2. The power supplied from the electric heater in manual mode is carefully adjusted from 0 % power and up until a steady temperature of about 100 °C is met.
3. The control valve is closed as fast but carefully to induce the lowest possible pressure. ( 350 kPa on low pressure side, 850 kPa on high pressure side)
4. The experiment is safely ended.

In the ETHEL model the resulting flow from the ETHEL experiment is replicated and the results are observed, i.e. the recorded effect in the ETHEL controller was used as an input in the model. The recorded mass flow rate in the experiment was used, but assumed constant, in the model.

### 5.2.2. System 1010 model

Decreasing the mass flow rate in the system 1010 model implies lowering the speed of the circulators. This is done for three different speeds, decreasing the speed from 80 % to 40 %, 50 % and 60 % respectively over three segments of 1000 seconds.

## 5.3. Experiment 2: Stop in intermediate coolant flow

### 5.3.1. ETHEL and ETHEL model

The ETHEL system heat exchanger is cooled by a water flow on the primary side, driven by a pump. To emulate a stop in flow on the primary cooling side of system 1010 we shut down the pump in the ETHEL system. However, because of the ETHEL equipment limits the heat may not increase beyond 35 °C on the compressor suction side, lest the compressor may be damaged. A very low temperature is therefore used in this case.

1. The system runs as normal. Data from relevant sensors are captured.
2. The power supplied from the electric heater in the manual mode is carefully adjusted from 0 % power and up until a steady temperature of about 50 °C is met.
3. The intermediate cooling system pump is turned off.
4. When the temperature between the heat exchanger and the compressor reaches 25 °C, the heater is turned off and the pump is turned on.
5. The experiment is safely ended.

In the ETHEL model the heat exchanger secondary circuit flow is redirected to free flow past the heat exchanger volume for some time, resulting in zero flow through the heat exchanger volume.

### 5.3.2. System 1010 model

Because of the zero-flow problem, the intermediate coolant flow in the system 1010 model could not be severely limited without serious interventions in the model structure. Therefore the flow in the secondary circuit was instead only decreased from the default 7.14 kg/s, 5.4 kg/s and 5.7 kg/s for W001, W002 and W003 respectively to 3 kg/s, first each on their own, then all heat exchangers at the same time. This was done for 1000 second intervals, with 1000 second in between.

## 5.4. Experiment 3: Increase in deposited target energy

### 5.4.1. ETHEL and ETHEL model

To impose a step in deposited effect into the ETHEL system in a safe manner the heat is increased gradually manually until desired output temperature is reached, then turned

off, then again turned on after a time. The experiment imposes minimal risks as the heat exchanger secondary side, and the compressor is running over time.

1. The system runs as normal. Data from relevant sensors are captured.
2. The power supplied from the electric heater in the manual mode is carefully adjusted from 0 % and up until a steady temperature of about 200 °C is met.
3. The heater is turned off. Wait until the system reaches a steady state.
4. The heater is turned on. Wait until the system reaches a steady state.
5. The experiment is safely ended.

In the ETHEL model the same effect is deposited by the electric heater as was during the ETHEL experiment, using the manual mode. The recorded mass flow rate in the experiment was used, but assumed constant, in the model.

### 5.4.2. System 1010 model

The two steps in the system 1010 model that induce effect in the wheel are introduced: first step to 2 MW for 1000 seconds, reduced to zero for 1000 seconds, then 1.5 MW for 1000 seconds.

## 5.5. Experiment 4: Heat step sensor test

### 5.5.1. ETHEL and ETHEL model

The sensor test is a simple step, using the electric heater built-in PID-controller. However, because of how the shut-off functions in the heater setup, a large integrator windup occurs, and one can expect large overshoots even from fairly low setpoints. Caution must therefore be taken not to overheat the system as the ultrasonic flowmeter is only specified to handle temperatures up to 250 °C.

1. The system runs as normal. Data from relevant sensors are captured.
2. Turn on the heater at 100 °C setpoint and wait until the system reaches a steady state.
3. Turn off the heater and wait until the system reaches a steady state.
4. Turn on the heater at 50 °C setpoint and wait until the system reaches a steady state.

5. The experiment is safely ended.

In the ETHEL model the same temperature set-points are used, and the PID-controller is set to the same parameters as the real PID-controller.

For this experiment there is no system 1010 model equivalent.

# Chapter 6.

# Results

All of the results from the experiments conducted on ETHEL have the corresponding event from the corresponding ideal sensor from the model in a dashed line.

## 6.1. Experiment 1

The resulting pressure, temperature, mass flow rate, and estimated percent of air for experiment 1 using air are presented in figure 6.1, figure 6.2, figure 6.3, and figure 6.4 respectively. The same plots using helium are presented in figure 6.5, figure 6.6, figure 6.7, and figure 6.8 respectively.

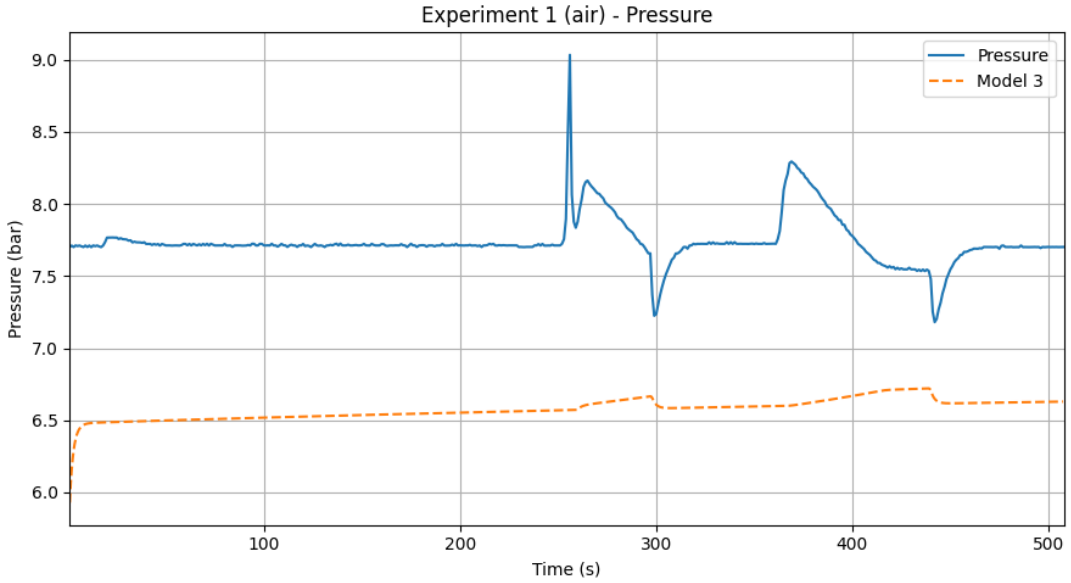


**Figure 6.1.:** Pressure for experiment 1 using air. Model in a dashed line.

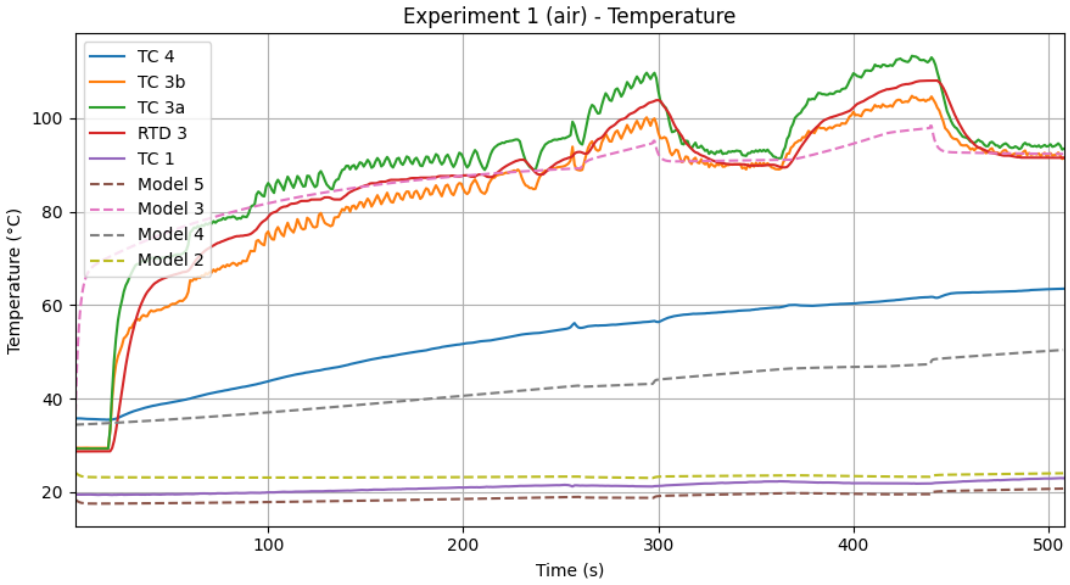


**Figure 6.2.:** Temperature for experiment 1 using air. Model in dashed lines.

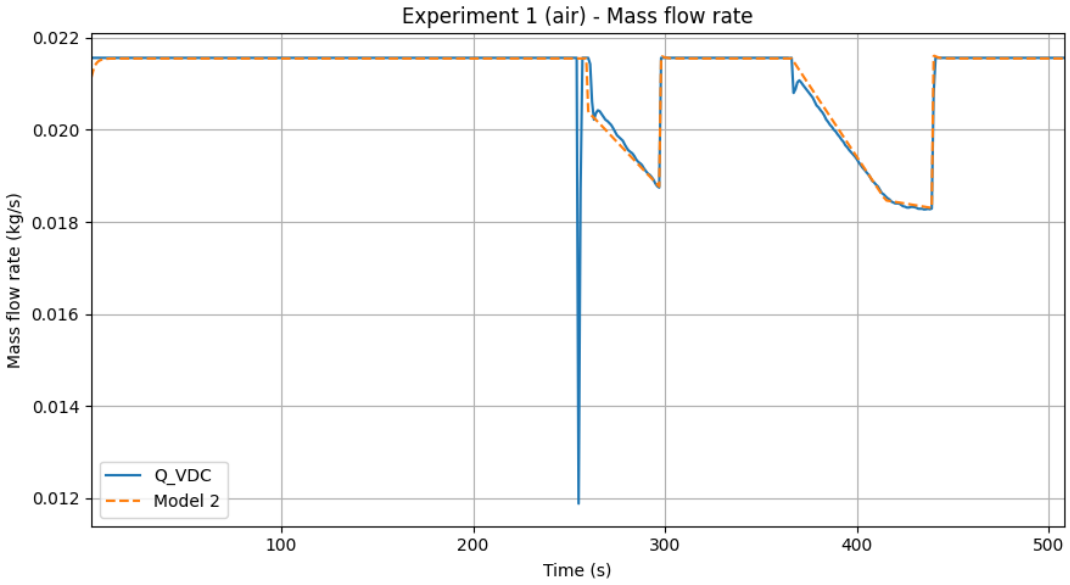


**Figure 6.3.:** Mass flow rate for experiment 1 using air. Model in a dashed line.

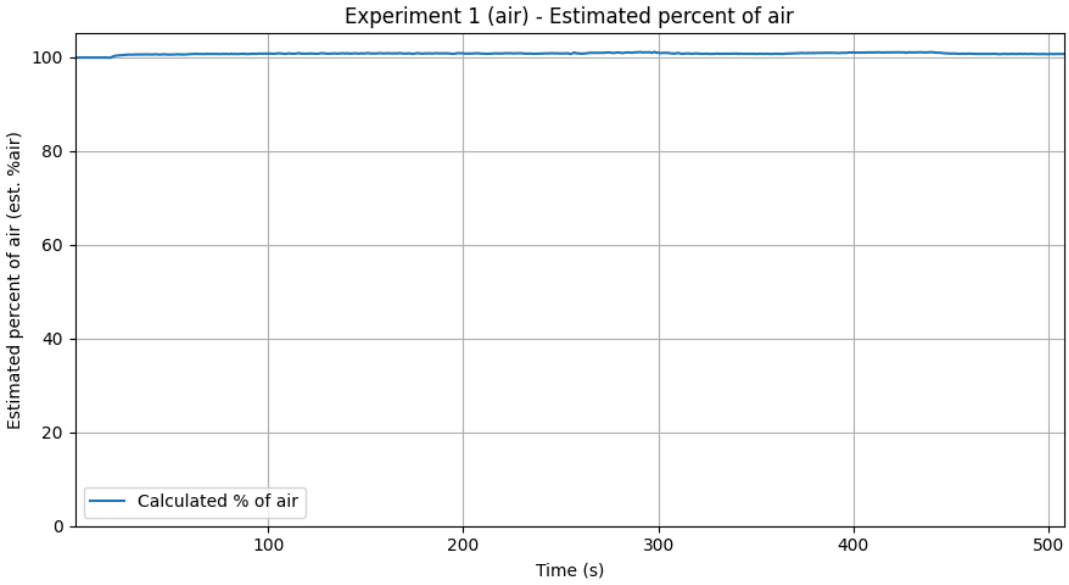


**Figure 6.4.:** Estimated percent of air for experiment 1 using air.

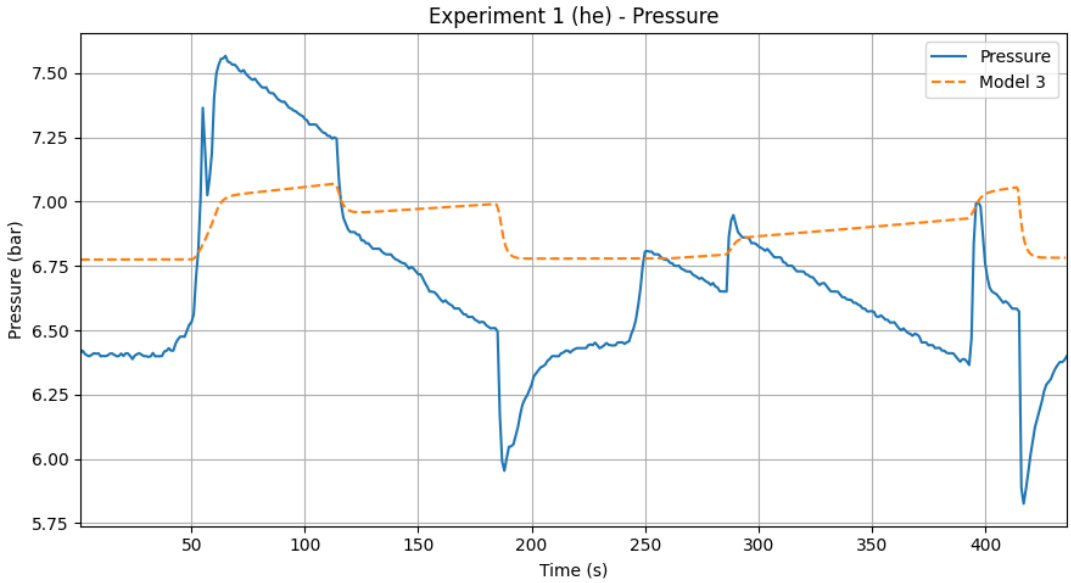


**Figure 6.5.:** Pressure for experiment 1 using helium. Model in a dashed line.

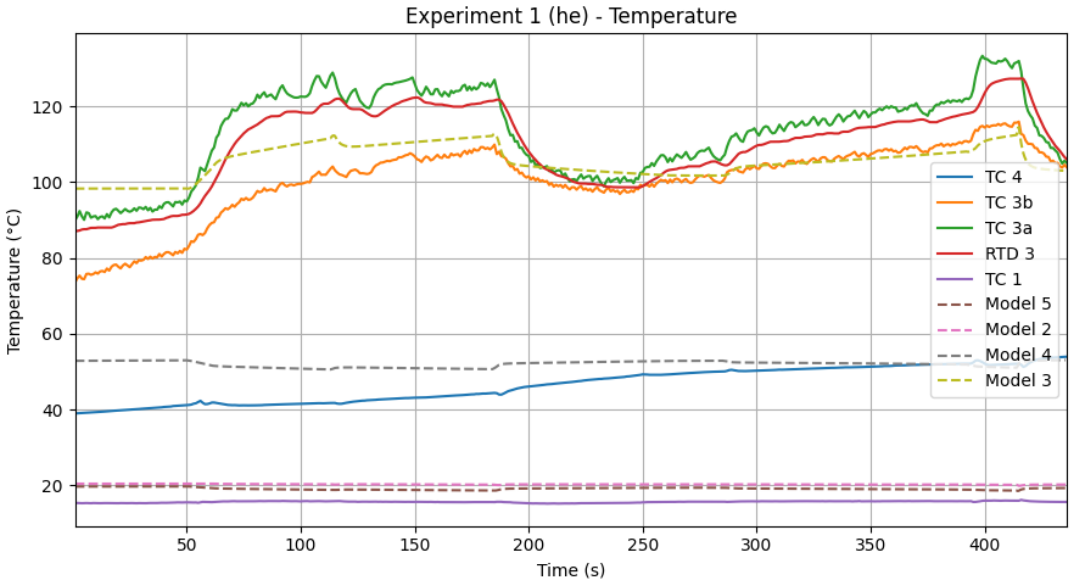


**Figure 6.6.:** Temperature for experiment 1 using helium. Model in dashed lines.

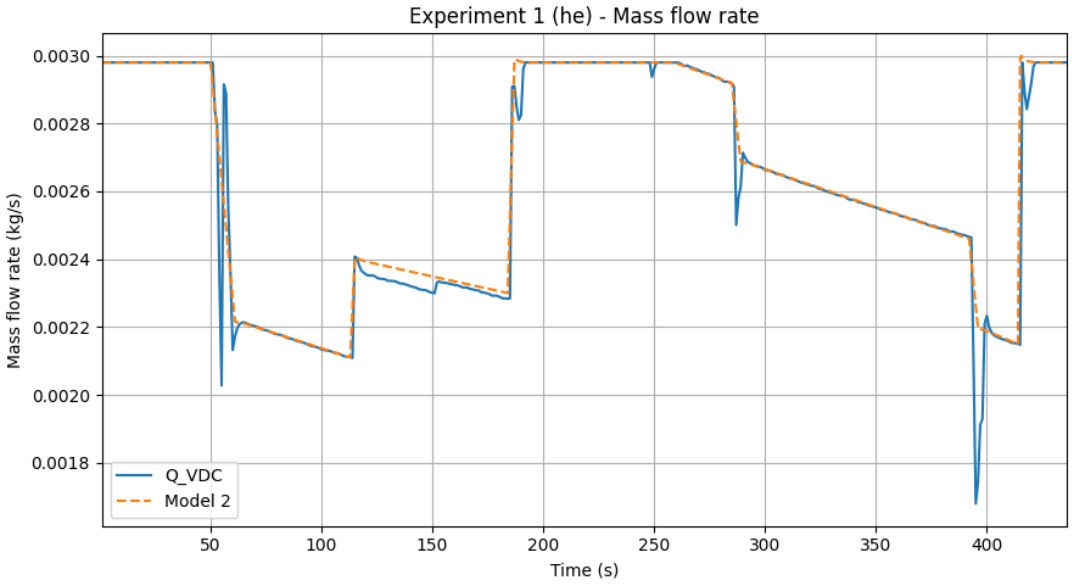


**Figure 6.7.:** Mass flow rate for experiment 1 using helium. Model in a dashed line.

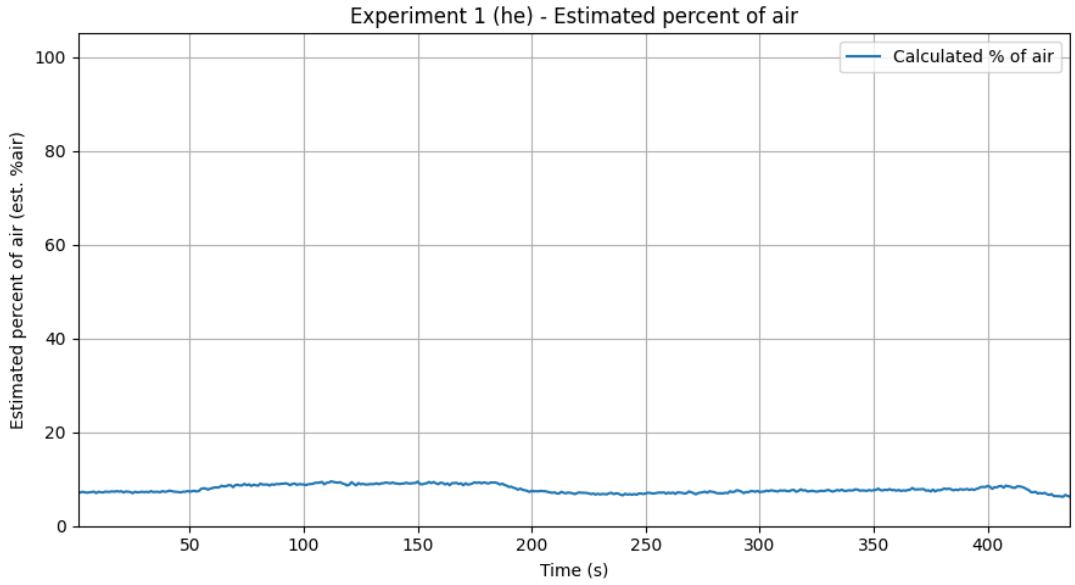


**Figure 6.8.:** Estimated percent of air for experiment 1 using helium.

### 6.1.1. Observations

In the experiment with air, close to 100 % air percentages are observed, which are fairly low (< 10 %) percentages in the experiment with helium.

In both experiments lowering the flow correlated with an increase in temperature in section 3, and a lowered temperature in section 4. Both phenomena are reflected in the model.

In both experiments ETHEL starts measurements at temperatures above room temperature (approximately 20 °C), as the model was.

The pressure in ETHEL in the experiment with air correlates poorly with the model behaviour. In the helium experiment the pressure is more similar between the model and ETHEL, however seldom contains the same amplitude or trends.

In the experiment with air the temperature in the model is at most points lower than ETHEL, and the same holds for location 3 in the experiment with helium.

## 6.2. Experiment 2

The resulting pressure, temperature, mass flow rate, and estimated percent of air for experiment 2 using air are presented in figure 6.9, figure 6.10, figure 6.11, and figure 6.12 respectively. The same plots using helium are presented in figure 6.13, figure 6.14, figure 6.15, and figure 6.16 respectively.

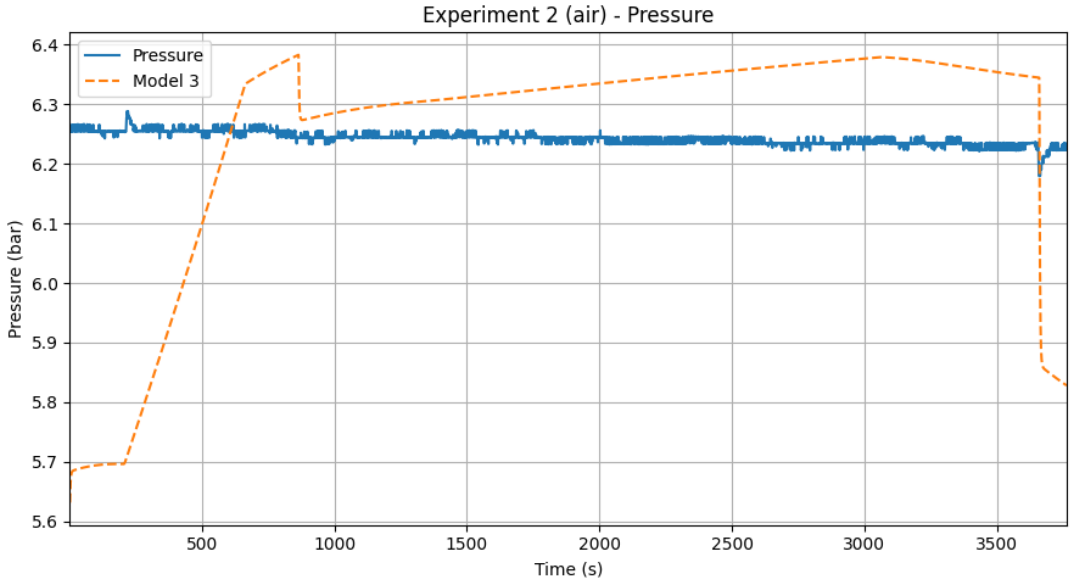


**Figure 6.9.:** Pressure for experiment 2 using air. Model in a dashed line.

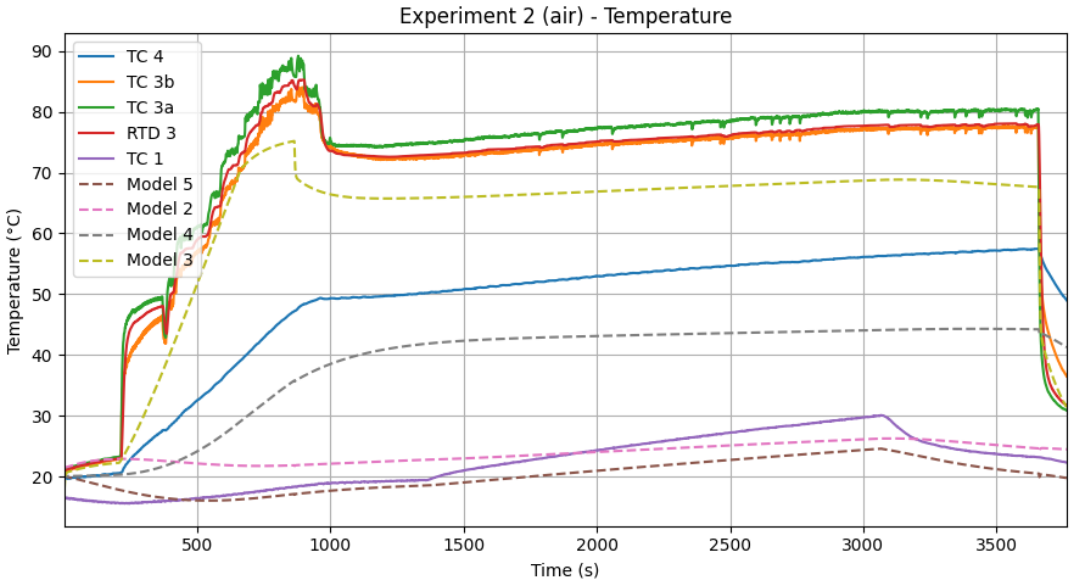


**Figure 6.10.:** Temperature for experiment 2 using air. Model in dashed lines.

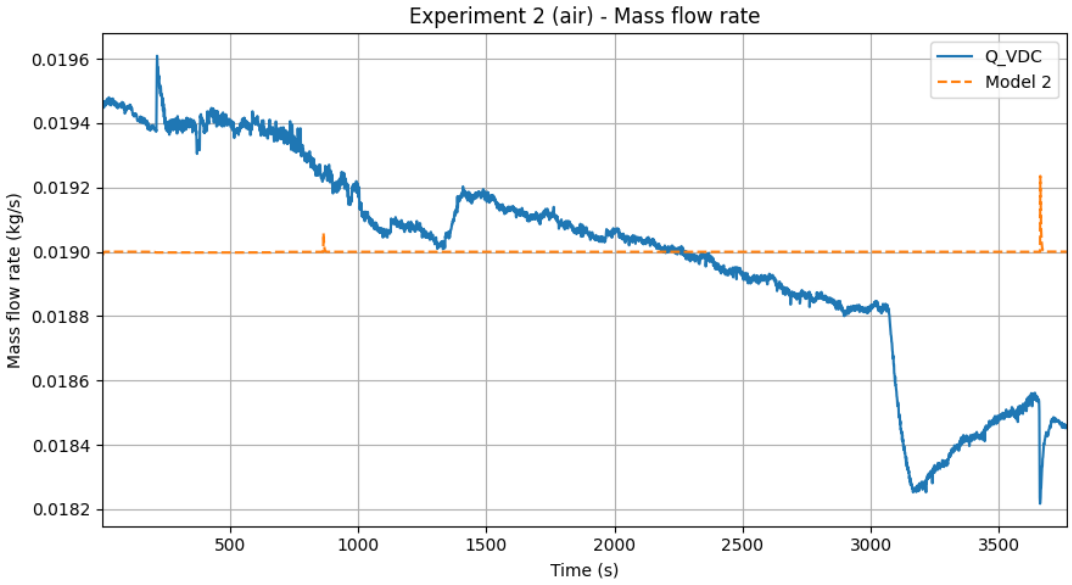


**Figure 6.11.:** Mass flow rate for experiment 2 using air. Model in a dashed line.

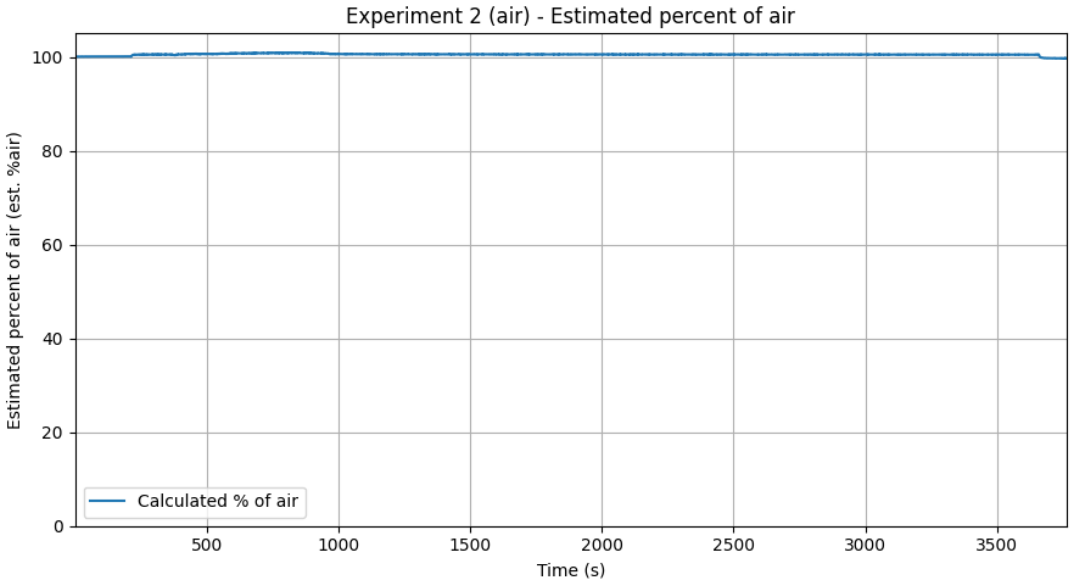


**Figure 6.12.:** Estimated percent of air for experiment 2 using air.

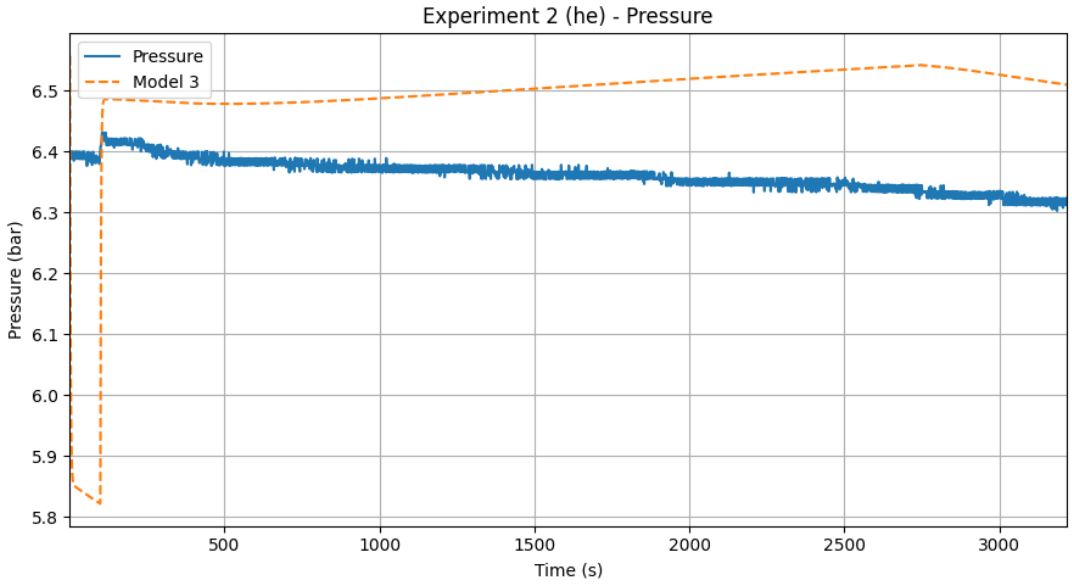


**Figure 6.13.:** Pressure for experiment 2 using helium. Model in a dashed line.

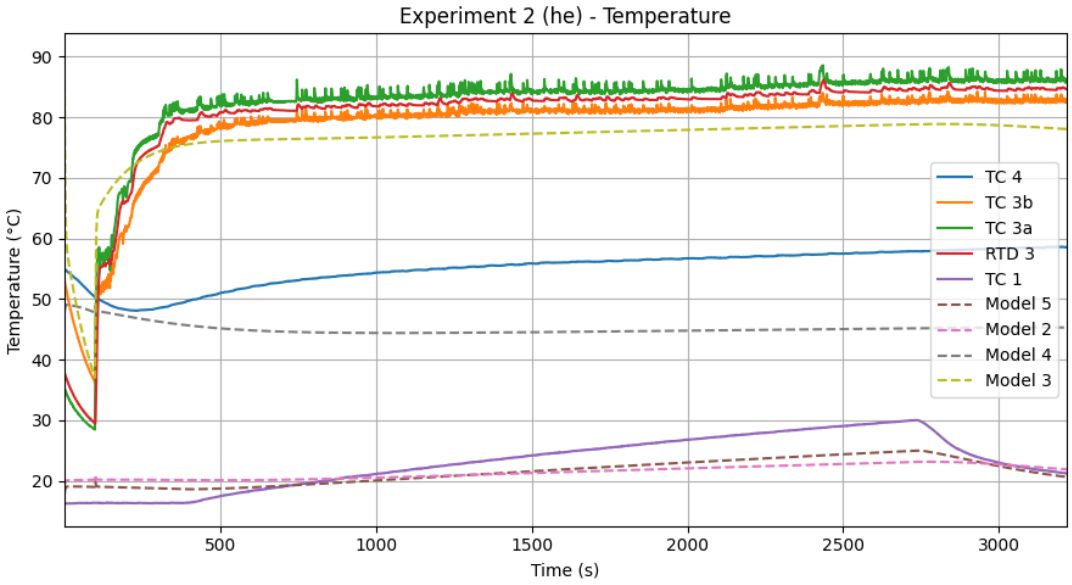


**Figure 6.14.:** Temperature for experiment 2 using helium. Model in dashed lines.

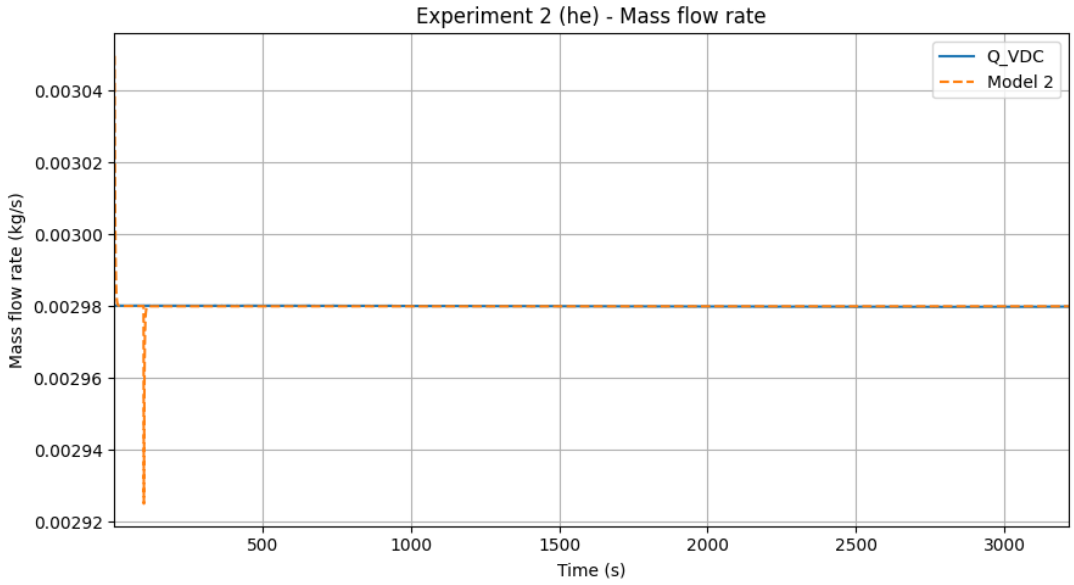


**Figure 6.15.:** Mass flow rate for experiment 2 using helium. Model in a dashed line.

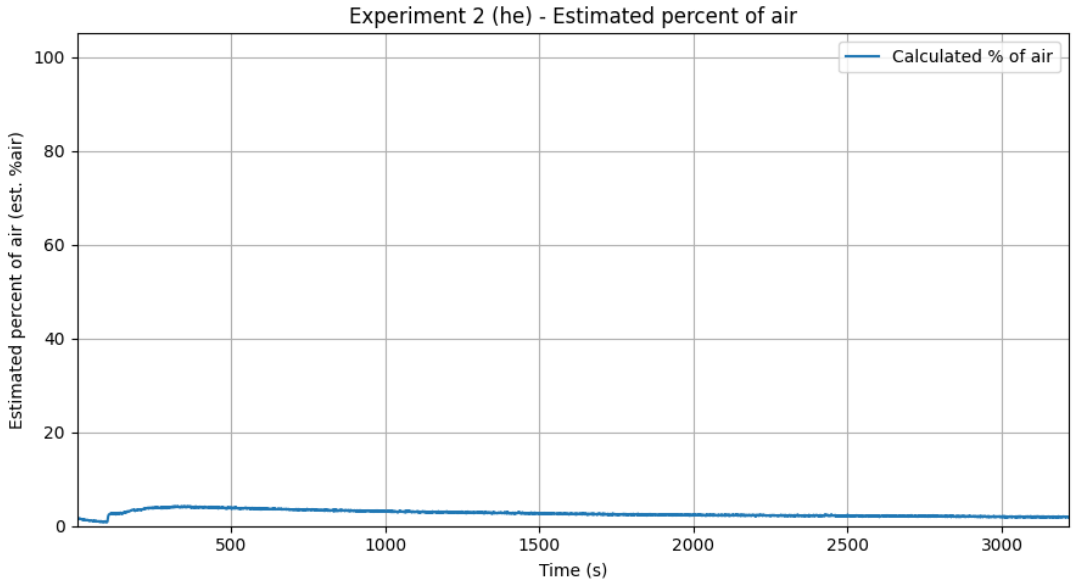


**Figure 6.16.:** Estimated percent of air for experiment 2 using helium.

### 6.2.1. Observations

In the experiment with air, close to 100 % air percentages are observed, which are very low (< 5 %) percentages in the experiment with helium.

The pressure in the experiment with air as medium demonstrates a stable behaviour as the model with air fluctuates relatively to temperature. Similarly the helium experiment results in a more stable pressure, in contrast to the model.

In both experiments the system was initialised as an above room temperature (hot) system, as the model was. The effects of turning off the secondary system are less impactful in the model than the real experiment data, for both mediums.

## 6.3. Experiment 3

The resulting pressure, temperature, mass flow rate, and estimated percent of air for experiment 3 using air are presented in figure 6.17, figure 6.18, figure 6.19, and figure 6.20 respectively. The same plots using helium are presented in figure 6.21, figure 6.22, figure 6.23, and figure 6.24 respectively.

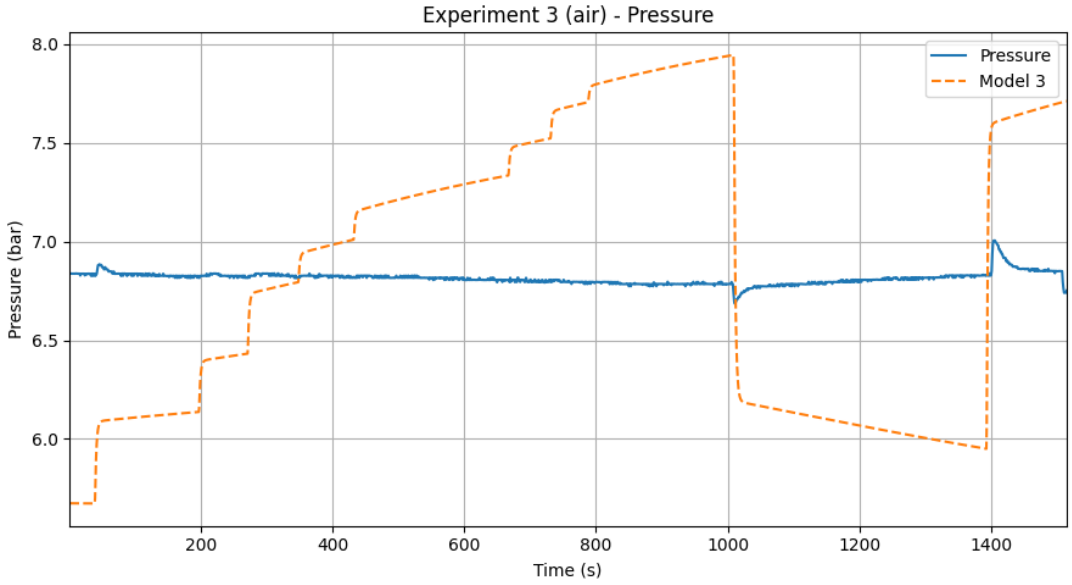


**Figure 6.17.:** Pressure for experiment 3 using air. Model in a dashed line.

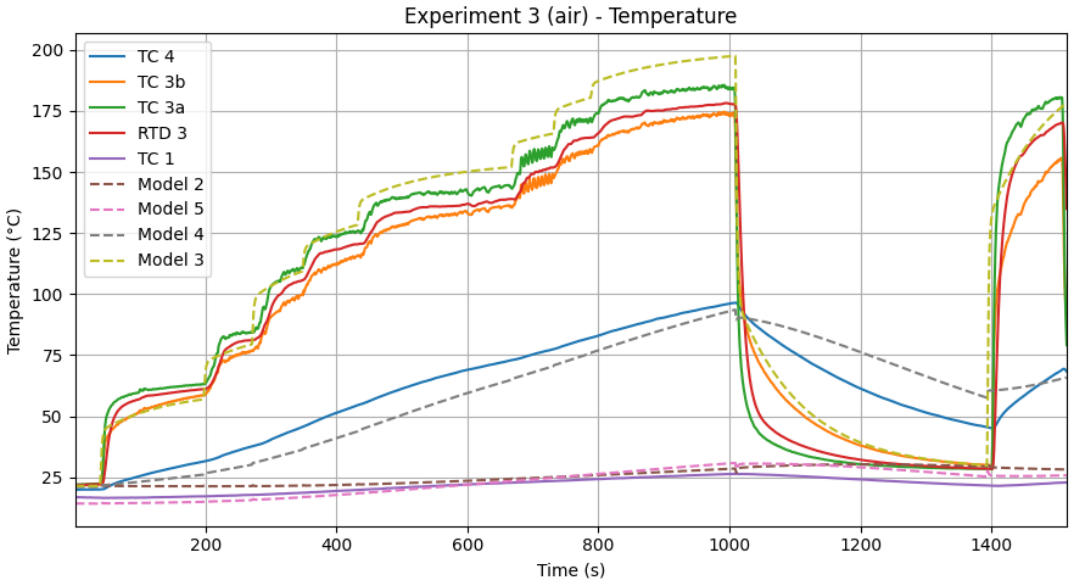


**Figure 6.18.:** Temperature for experiment 3 using air. Model in dashed lines.

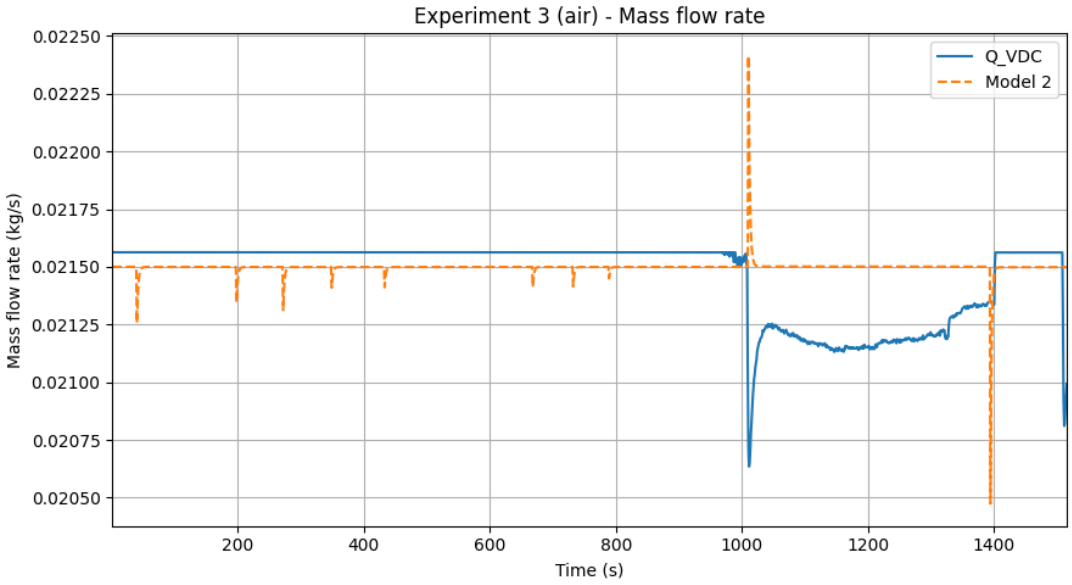


**Figure 6.19.:** Mass flow rate for experiment 3 using air. Model in a dashed line.

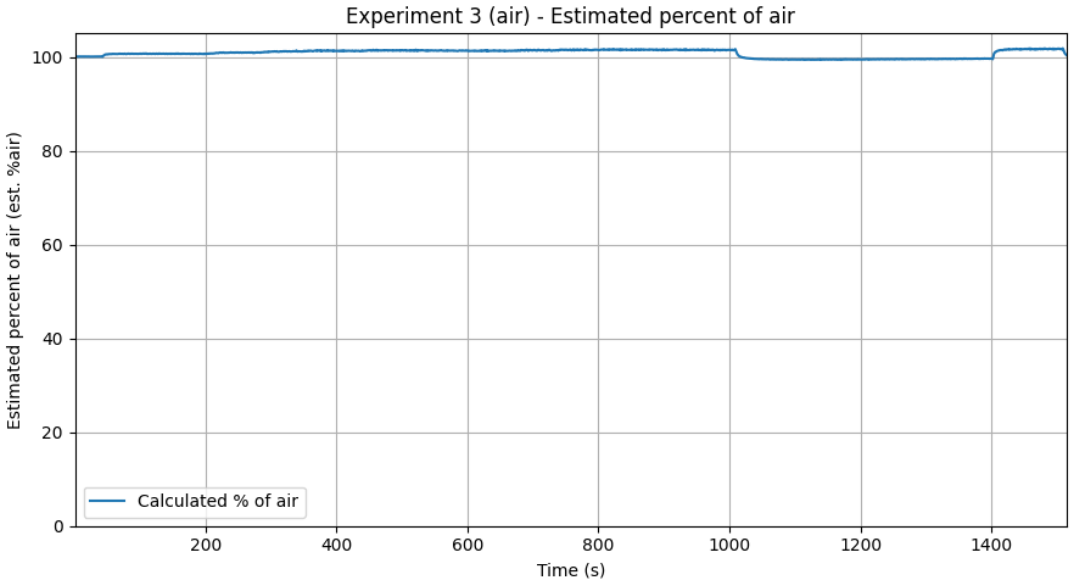


**Figure 6.20.:** Estimated percent of air for experiment 3 using air.

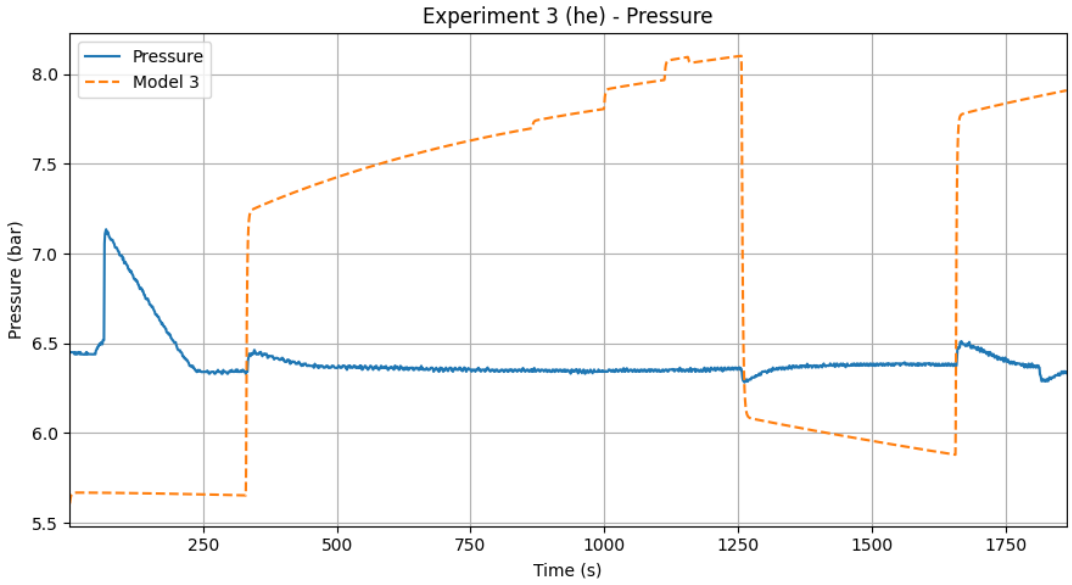


**Figure 6.21.:** Pressure for experiment 3 using helium. Model in a dashed line.

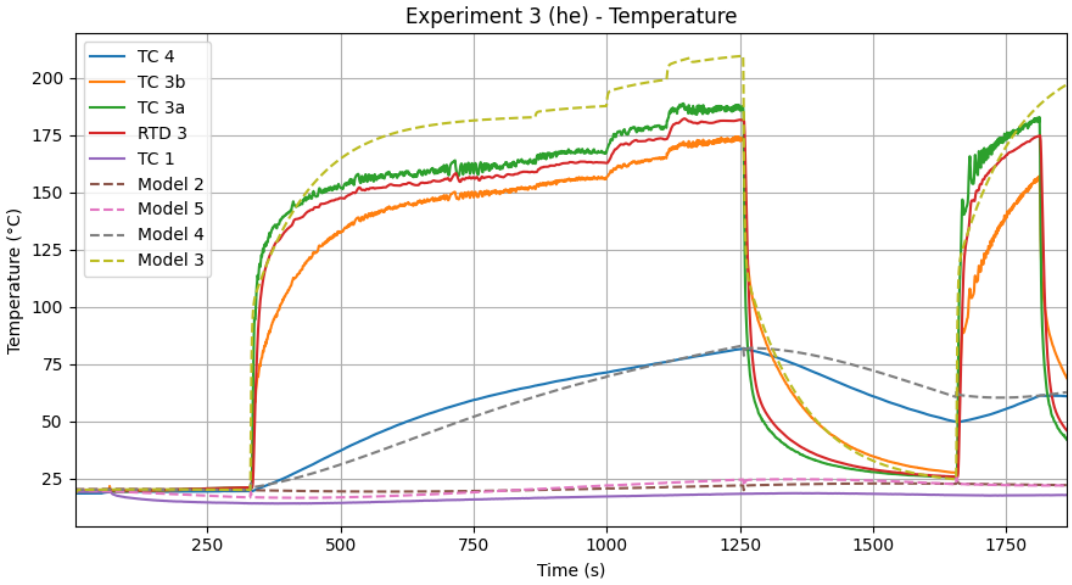


**Figure 6.22.:** Temperature for experiment 3 using helium. Model in dashed lines.

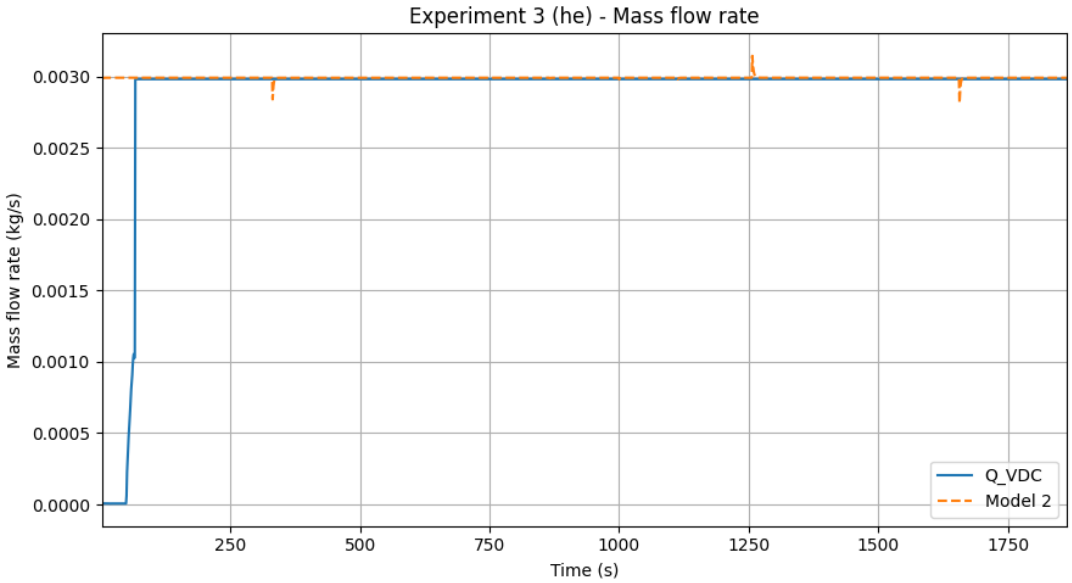


**Figure 6.23.:** Mass flow rate for experiment 3 using helium. Model in a dashed line.

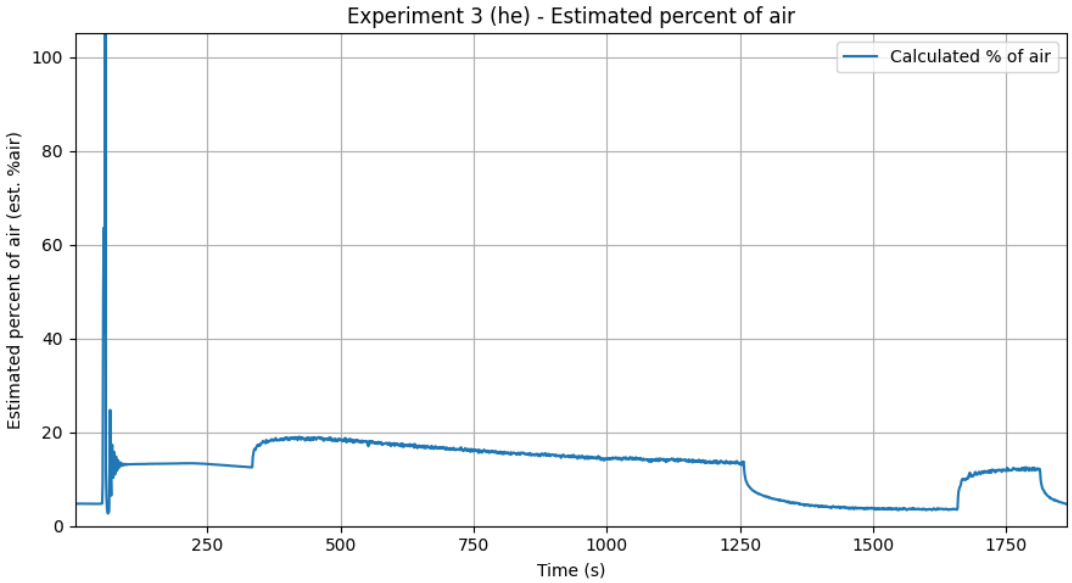


**Figure 6.24.:** Estimated percent of air for experiment 3 using helium.

### 6.3.1. Observations

In the experiment with air, close to 100 % air percentages are observed; however, quite high amounts of air ( 20 %) percentages were found in the experiment with helium.

## 6.4. Experiment 4

The resulting pressure, temperature, mass flow rate, and estimated percent of air for experiment 4 using air are presented in figure 6.25, figure 6.26, figure 6.27, and figure 6.28 respectively. The same plots using helium are presented in figure 6.29, figure 6.30, figure 6.31, and figure 6.32 respectively.

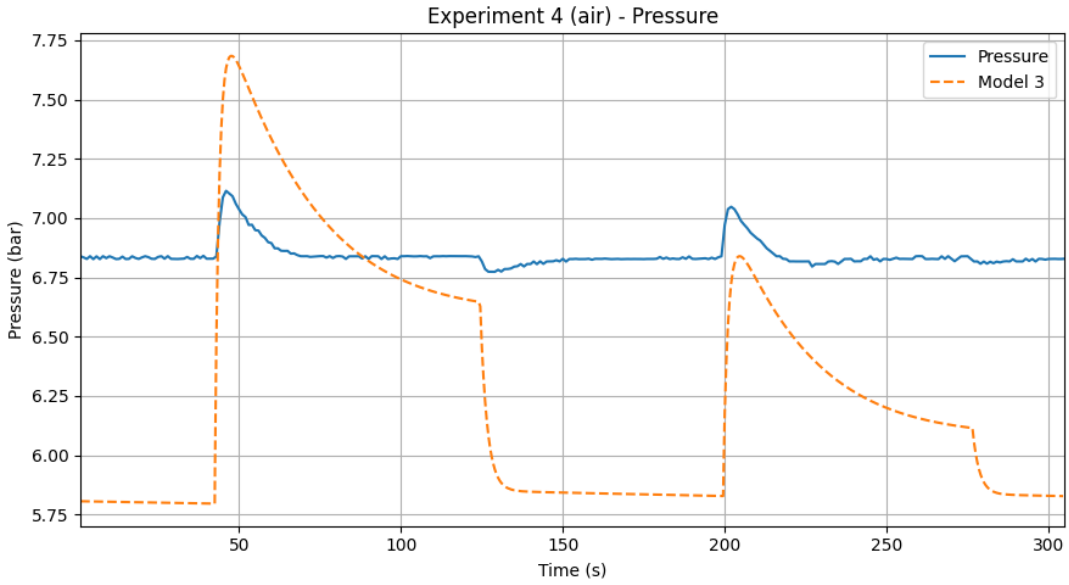


**Figure 6.25.:** Pressure for experiment 4 using air. Model in a dashed line.

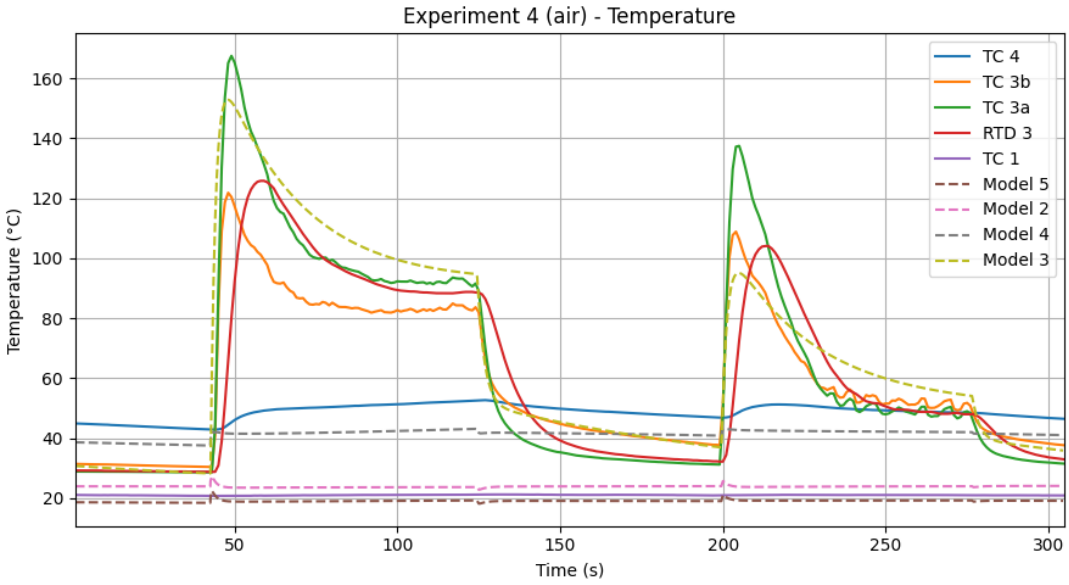


**Figure 6.26.:** Temperature for experiment 4 using air. Model in dashed lines.

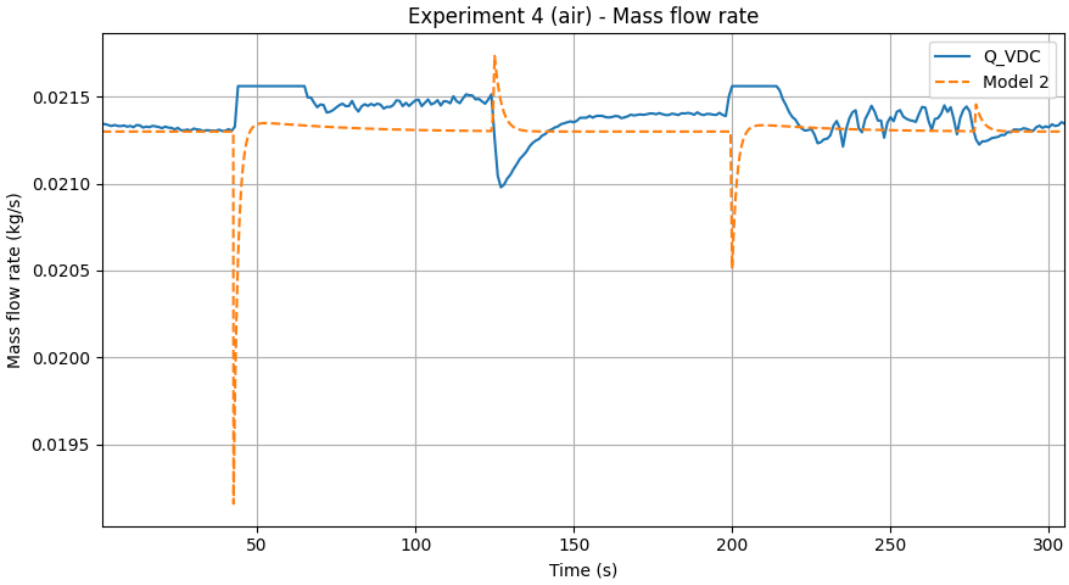


**Figure 6.27.:** Mass flow rate for experiment 4 using air. Model in a dashed line.

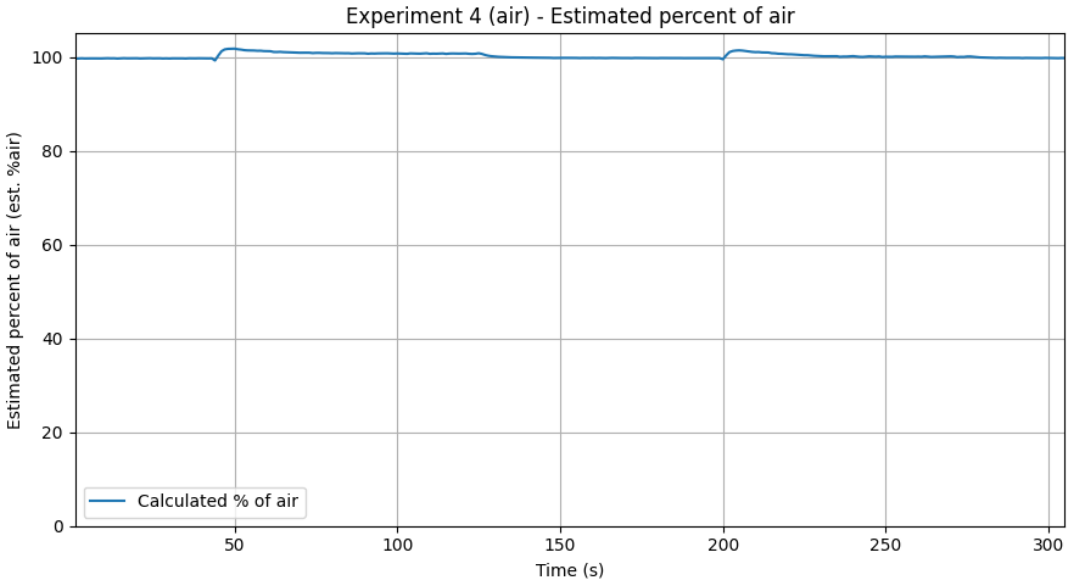


**Figure 6.28.:** Estimated percent of air for experiment 4 using air.

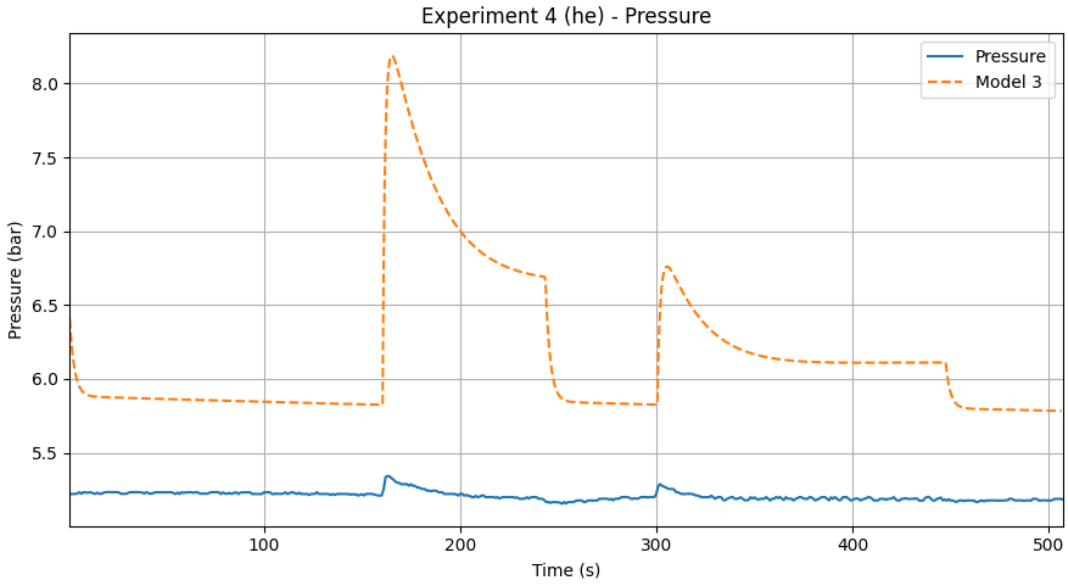


**Figure 6.29.:** Pressure for experiment 4 using helium. Model in a dashed line.

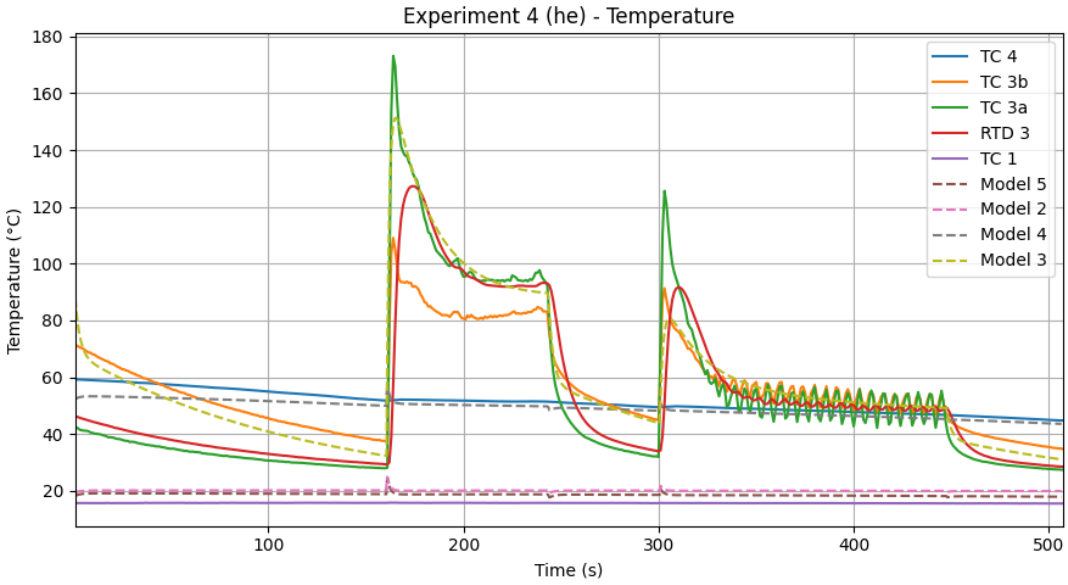


**Figure 6.30.:** Temperature for experiment 4 using helium. Model in dashed lines.

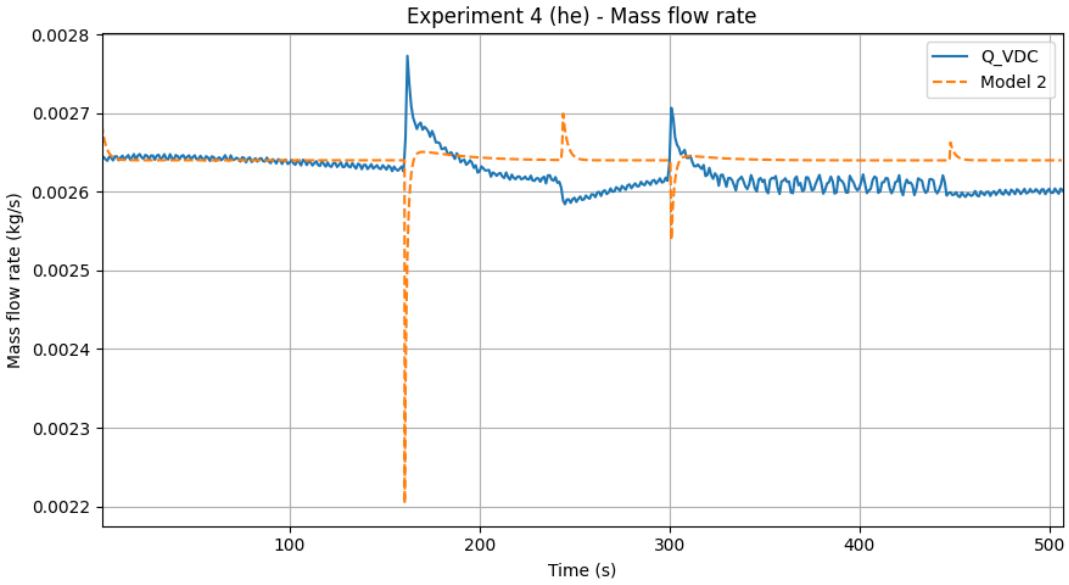


**Figure 6.31.:** Mass flow rate for experiment 4 using helium. Model in a dashed line.

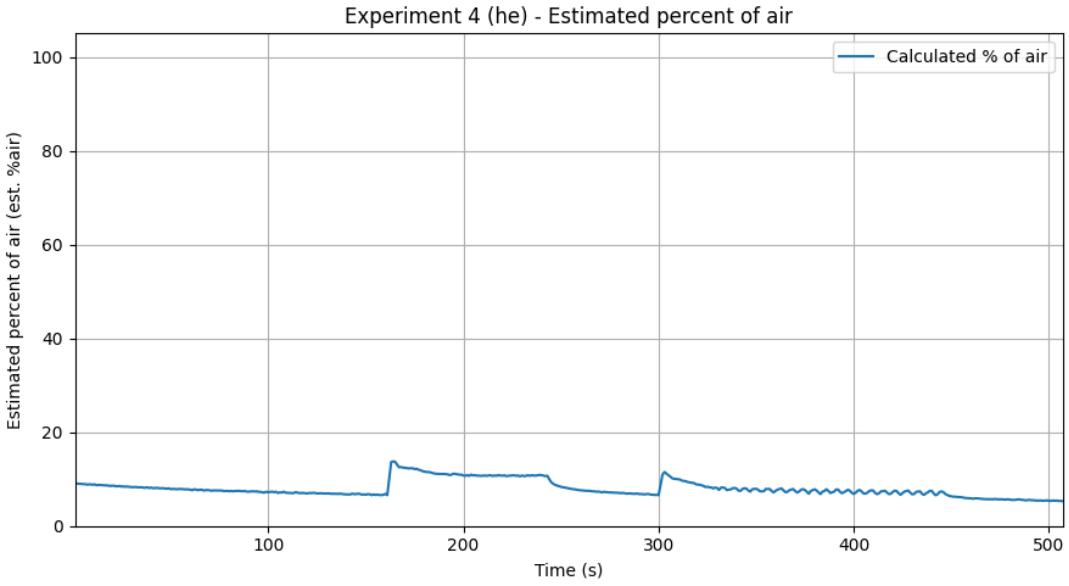


**Figure 6.32.:** Estimated percent of air for experiment 4 using helium.

### 6.4.1. Observations

In the experiment with air, close to 100 % air percentages are observed; however, fairly high amounts of air ( 15 %) percentages were found in the experiment with helium.

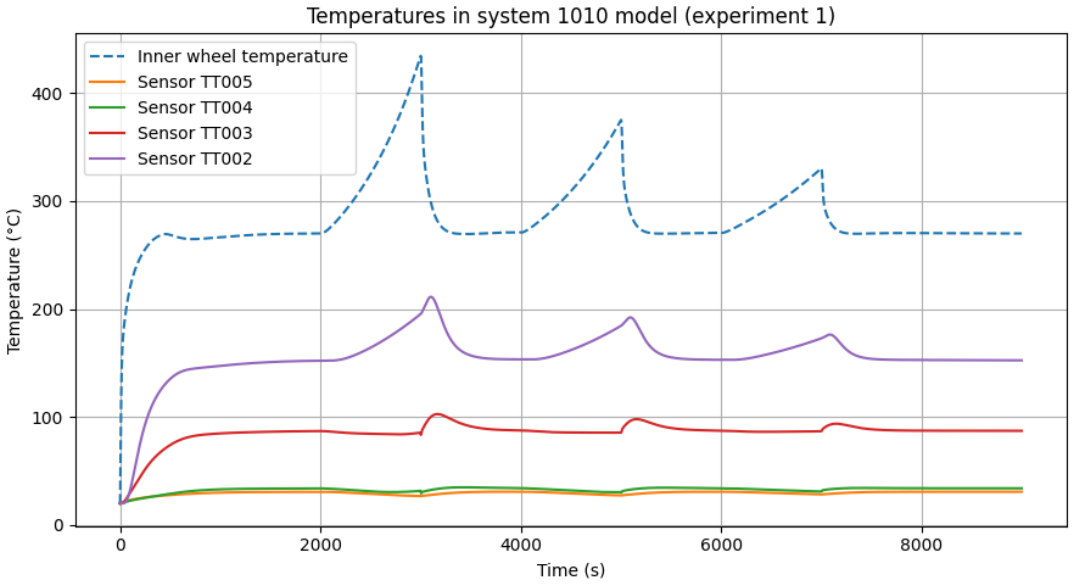


**Figure 6.33.:** Temperature for the system 1010 model when emulating experiment 1.

A high overshoot in the temperatures in both experiments is observed before the temperature stabilises at the set-point. Furthermore, even after stabilisation, the temperature experiences fast oscillations, especially around the second step.

## 6.5. System 1010 model results

The results of the event for the system 1010 model corresponding the experiments are presented in figures 6.34 and 6.33 for experiment 1, figures 6.36 and 6.35 for experiment 2, and figures 6.38 and 6.37 for experiment 3.

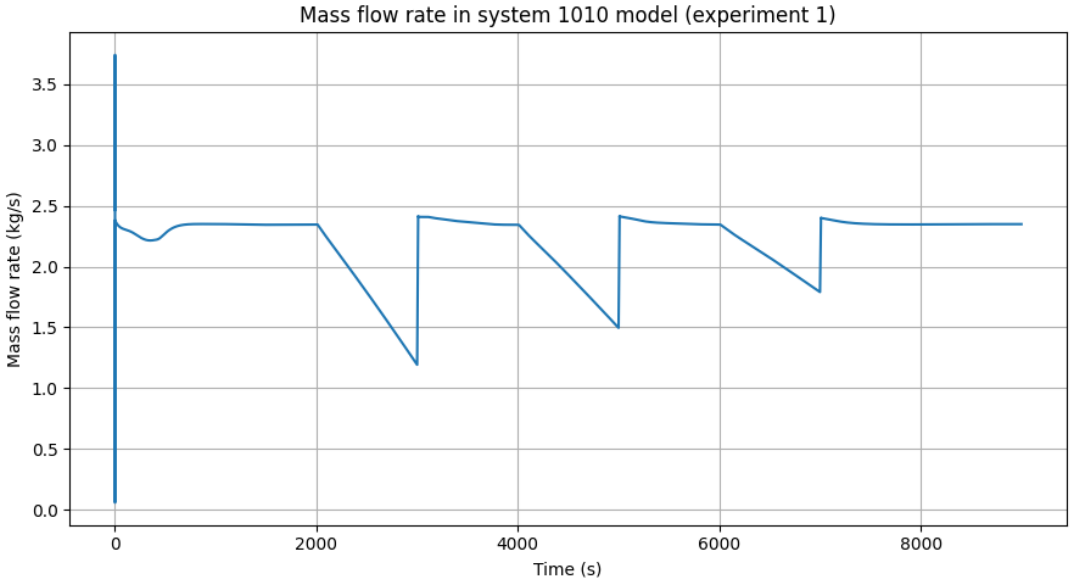


**Figure 6.34.:** Mass flow rate for the system 1010 model when emulating experiment 1.

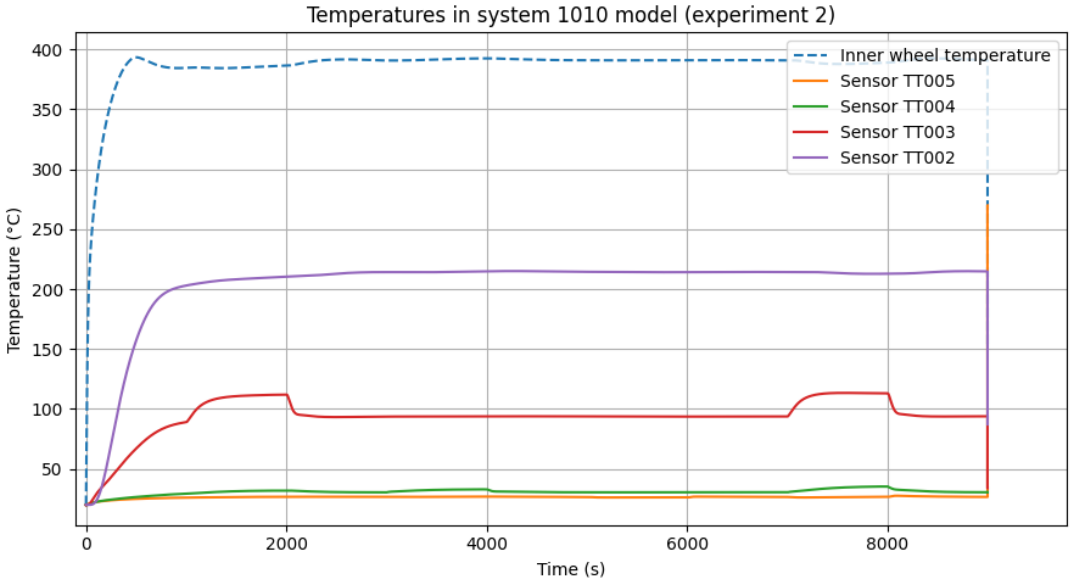


**Figure 6.35.:** Temperature for the system 1010 model when emulating experiment 2.

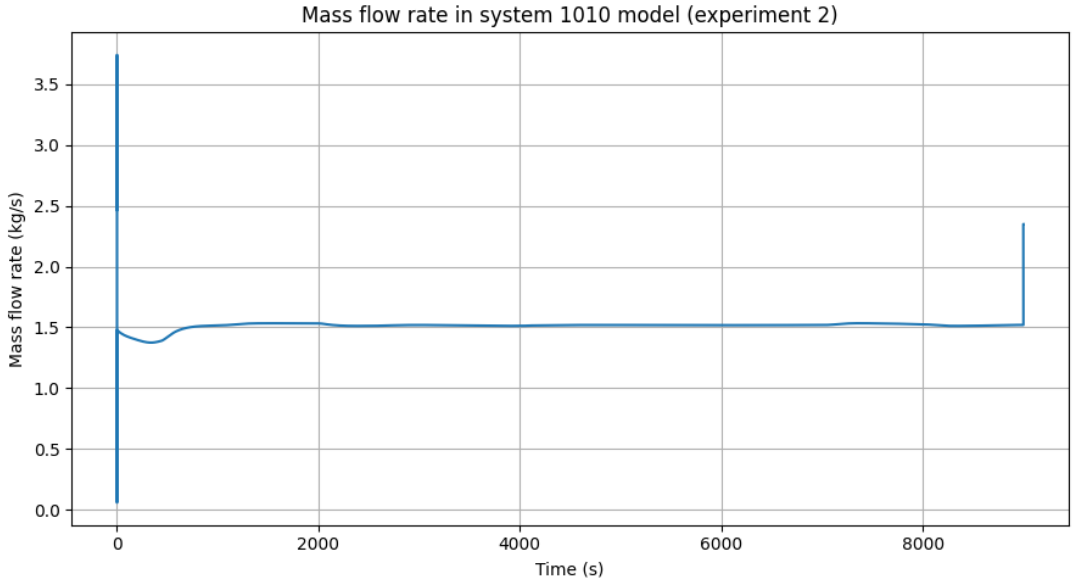


**Figure 6.36.:** Mass flow rate for the system 1010 model when emulating experiment 2.

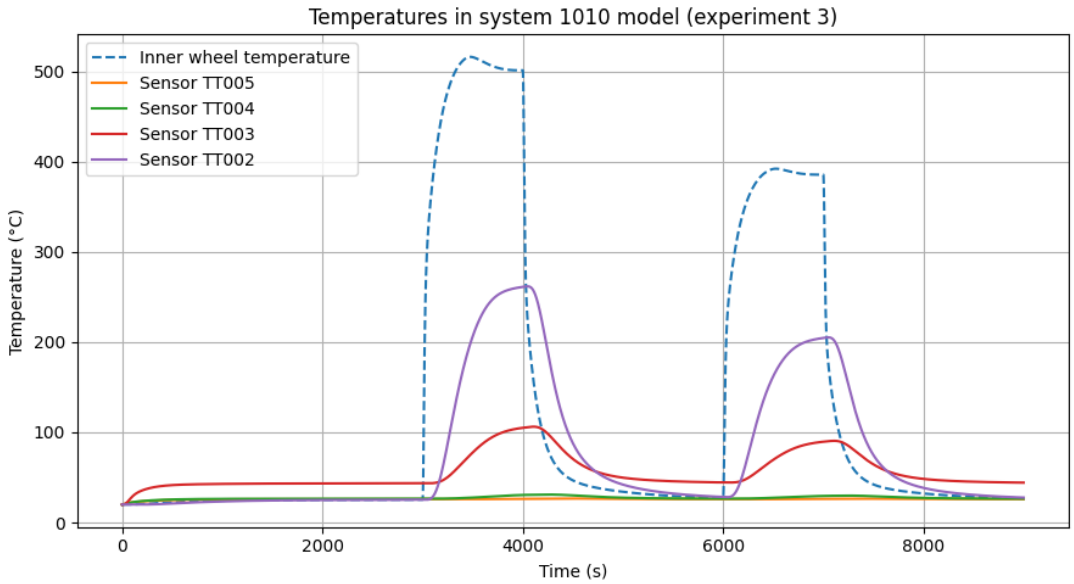


**Figure 6.37.:** Temperature for the system 1010 model when emulating experiment 3.

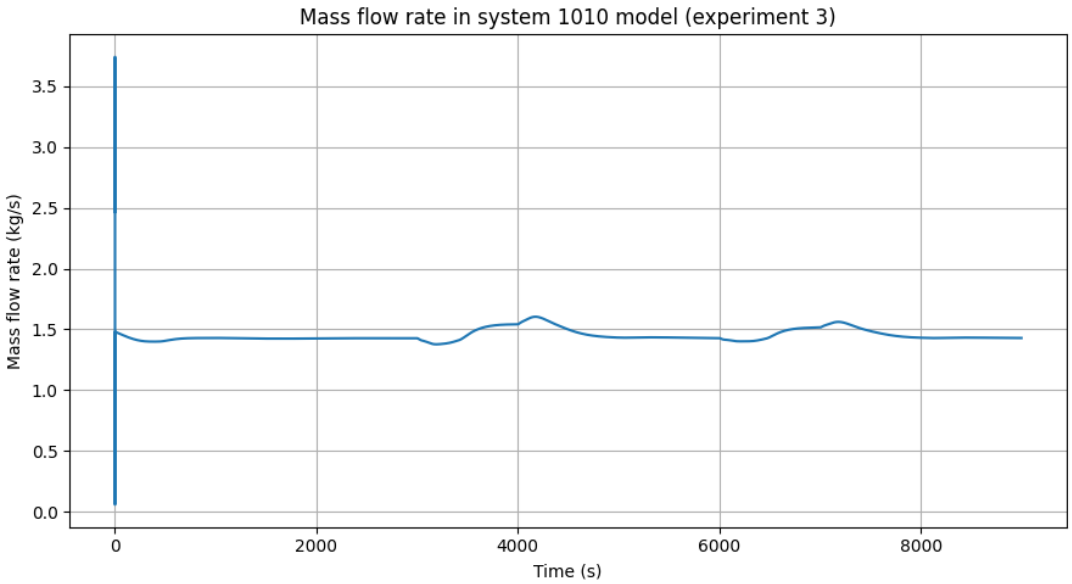


**Figure 6.38.:** Mass flow rate for the system 1010 model when emulating experiment 3.

# Chapter 7.

# Analysis

## 7.1. Model evaluation

### 7.1.1. Error and correlation analysis

In the error and correlation analysis data from the model output and real output will be used. Only at two points do the systems share a temperature measuring location, and is therefore worth using for analysis. These points are at location 3, and location 4. For brevity only the data from location 3 will be used, though the conclusions made for location 3 is assumed to extend to the whole system.

The fit of the model compared to the corresponding real data in location 3 was calculated according to the method described in section 2.2. The results are a NRMSD of 0.20 corresponding to a fit of 80 % in experiment 1, a NRMSD of 0.09 corresponding to a fit of 91 % in experiment 2, a NRMSD of 0.20 corresponding to a fit of 80 % in experiment 3, and a NRMSD of 0.15 corresponding to a fit of 85 % in experiment 4. The analysis yielded positive results, a fit of over 80 % in all cases implies a fairly good performance of the model. The error will however be investigated further.

In figure 7.1 the absolute error between the model and the real system for location 3, relative to the momentary measured temperature, is shown. The plot demonstrates a large momentary error in some specific locations, up to 300 % of the current temperature in experiment 3. Calculations show, however, that the mean relative error for all experiments is 10.1 %.

In figure 7.2 the normalised cross-correlation between the model and the system output is presented. The plot demonstrates a large peak at zero lag, which is an indicator of a good correlation. There is however some oscillations or disturbances at other lags, which reaches up to an absolute value of 0.5, meaning the results of this analysis is not conclusive.

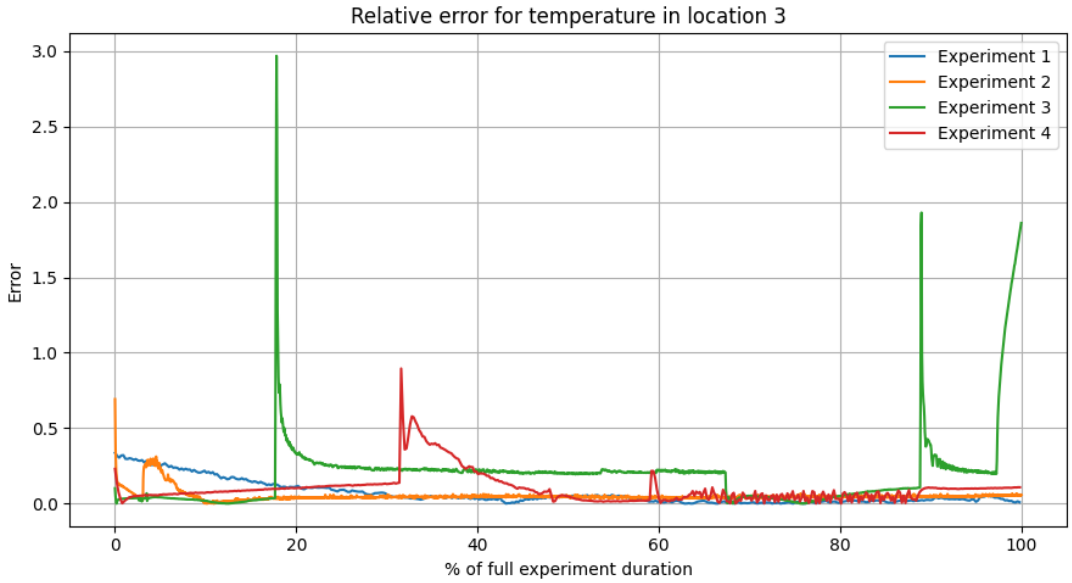


**Figure 7.1.:** Relative error between model and real data for each experiment at location 3.

In figure 7.3 a scatter plot is presented where the points represent the output from the model on the y-axis and the real output on the x-axis, normalised over their full range. A straight line has been fitted to the data using the least-squares method, and the slope is 0.818. As explained in section 2.2, the Pearson correlation factor must therefore be just 0.818, and this implies that the model has a strong positive correlation to the real system output.

From the conducted analysis we conclude that the time-response behavior is good, although worth noting that outliers, such as represented in figure 7.3 as points far away from the straight line, may skew the results. Leading to large oscillations and peaks seen in figure 7.2.

### 7.1.2. Discretisation of volumes

In experiment 2, the secondary circuit in the heat exchanger was stopped, effectively stopping the flow of water through the heat exchanger volume. In the real experiment the stationary water volume would create hot spots closest to the primary pipes, filled with flowing hot gas.

However, in the model the heat volume is discretised, i.e. it is seen as a single unit of temperature, pressure, flow, et.c. The model volume could be seen as a perfectly mixed volume of a single temperature. Because of this it is safe to assume less cooling occurs

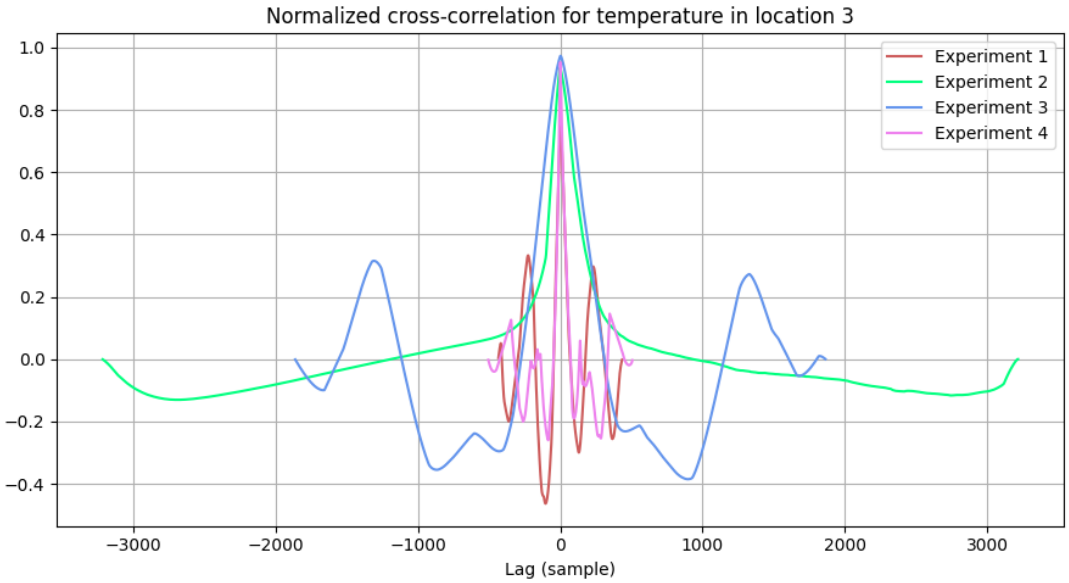


**Figure 7.2.:** Normalised cross-correlation between model output and real output.

between the real volume and the gas, than between the model volume and the gas. The local difference between the temperature in the volume and the gas in the real case is lower, and therefore the thermal flow is lower, see 2.8.

### 7.1.3. Losses and estimations

The estimated percent of air for all experiments conducted with air relays an amount of air close to 100 %, which implies that the estimation is fair, at least for high percentages of air. However, one can assume that the estimation is worse with large percentages of helium, as the heat transfer coefficient for helium is higher, thereby increasing the losses between the thermocouple and the ultrasonic flowmeter, as per equation 2.8 (see section 2.4).

Furthermore, while estimating the amount of air in the real system temperature losses lead to misleading results. For example, in any given experiment an increasing amount of estimated air is observed to be correlating to increasing temperatures; however, it is unlikely that the amount of air in the system increase at any point of the experiment. The reason being that the system is pressurised, induced by a pressure controlling valve from a helium tank. Instead, this points to increased losses induced by a higher temperature and the thermal transfer rate being dependent on the difference in temperature, as seen in equation 2.8. In turn the higher losses leads to a difference in temperature between the point where the temperature is measured, and the point where the speed of sound in the medium is measured. The result is a misleading calculation of the percent of air as per

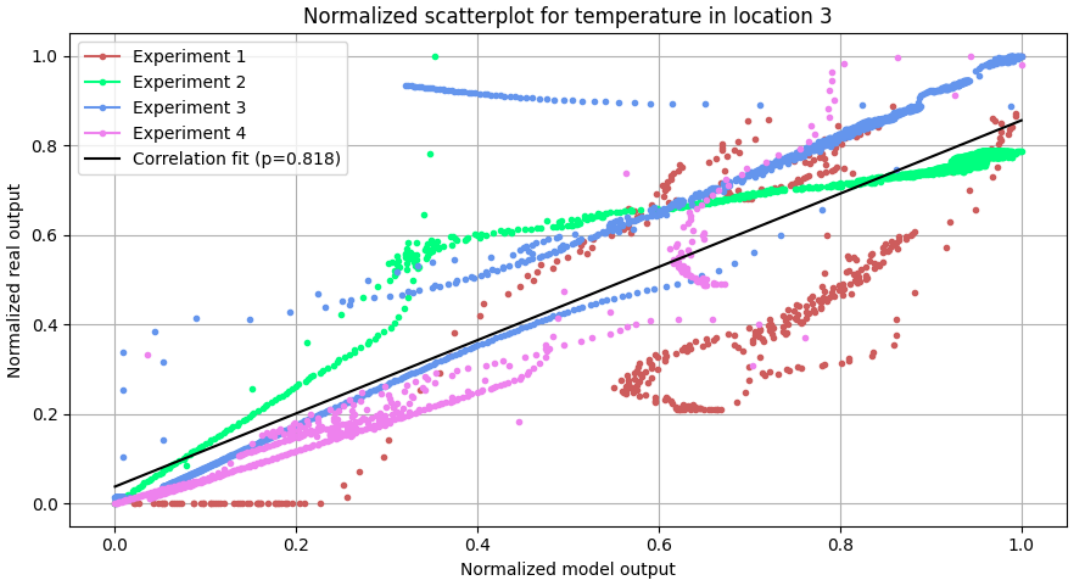


**Figure 7.3.:** Scatter-plot of normalised model and real output, and best fit straight line.

equations 2.5 and 2.7.

### 7.1.4. Unmodeled features

In the ETHEL system the pressure control from the supplied air or helium was avoided, because of uncertainties in the control function and set-point. However, this may have affected the pressure, as the model pressure was seldom correlating with its measured counterpart. The pressure, in turn, may have affected the temperatures in unexpected ways and may account for some of the errors in the model data.

## 7.2. System identification and sensors

### 7.2.1. Sensor location

From the system 1010 model experiment 3 simulation data for temperatures in the system in two steps in effect are presented. The resulting temperatures are dependent on the input effect applied to the wheel.

Three locations are of interest: the temperature inside the hottest part of the target wheel;

the temperature in sensor T002, the first sensor after the target wheel; and the temperature in a pipe halfway from the target wheel to the first sensor. The latter location is just upstream of the filter, and the location is investigated to explore the sensor location, i.e. if the sensor time response would be improved depending on the sensor location to any discernible degree.

To identify the time-response of the temperature in these three locations one can use the methods described in section 2.5, see Matlab code in appendix B.

The results of the delay estimation are 0 samples for the wheel temperature, 40 samples (i.e. 20 seconds at sample frequency 2 Hz) for sensor TT002, and the same 40 samples for the prefilter location. The target wheel is directly supplied with heat, whereas sensor TT002 and the pre-filter pipe are further downstream of the helium flow. This implies the results are reasonable.

Interestingly there is no difference in a dead-time delay between the pre-filter location and sensor T002. This implies that the delay is caused by the target wheel specifically, and not the pipe segments.

Further the transfer functions for the given data, and delays were estimated, both were estimated as continuous transfer functions with one pole and no zeroes. The target wheel temperature transfer function had a pole in -0.01323 and a fit of 81.5 %, the TT002 temperature transfer function had a pole in -0.001968 and a fit of 77.4 %, and the pre-filter transfer function had a pole in -0.02693 and a fit of 74.5 %. The fit is fair, over 74 % in all cases, considering a transfer function with only one pole being a broad generalisation of the complex model. The step response for the transfer functions are presented in figure 7.4.

From the poles and the step response plot its deduced that the pre-filter transfer function is somewhat faster, implying a faster convergence to steady state beyond the dead-time of ca. 20 seconds. Most likely the slower system is caused by the larger section of piping between the points of measurement, and the target wheel, from which the hot helium originates. Interestingly the gain of the transfer function for the sensor is higher than the corresponding gain for the pre-filter location. This may be symptomatic of estimation errors in the system identification process.

### 7.2.2. Sensor types

Three temperature sensor types were used in the experiments on ETHEL: thermocouple sensor, resistance temperature detector, and an ultrasonic flowmeter. The latter ultrasonic

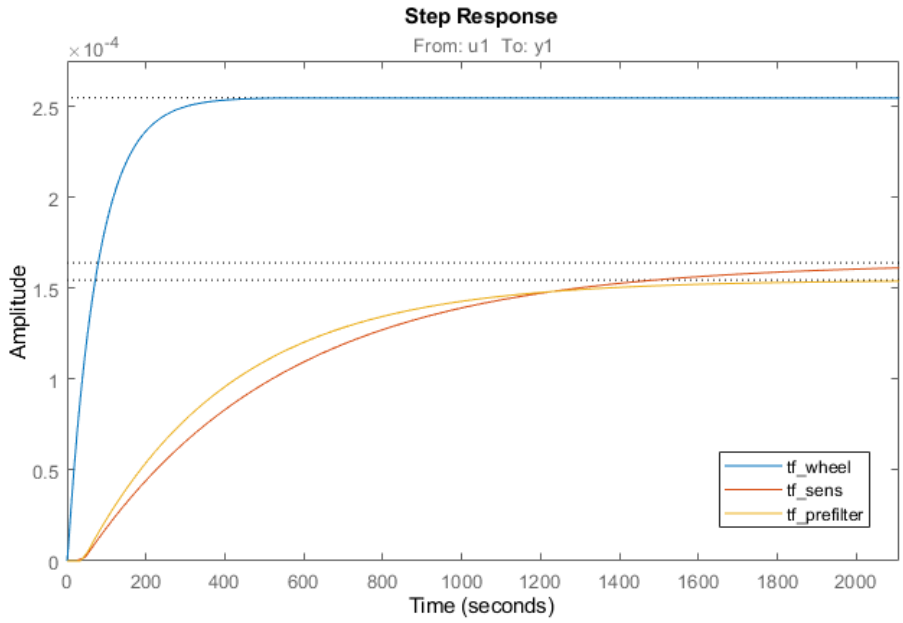


**Figure 7.4.:** Step plot of estimations for transfer functions from sensor TT002 (tf_sens), the pre-filter pipe (tf_prefilter), and the target wheel (tf_wheel), from the system 1010 model.

flowmeter does not measure temperature directly but rather the speed of sound in the medium. The speed of sound, however, can be used in equation 2.5 to derive the temperature, if the exact content of the fluid is known. Therefore for this section only the experiments with air will be examined, as the mix of air and helium in the helium experiments is derived from the speed of sound, and the equation would have an over dependence on that variable.

Experiment 4 was formulated with the expressed purpose to examine the performance of the sensors, however, when conducted demonstrated some unwanted behaviors. Using the automatic mode of the electric heater controller resulted in large overshoots and oscillations, furthermore the input is unknown or uncertain for the whole section. Therefore for this section the results from experiment 3, which resulted in a simple step function, will be used in determining the sensor speed.

The sensors are arranged over a distance in the ETHEL helium loop. There is however a thermocouple sensor close to the RTD sensor, as well as close to the ultrasonic flowmeter. The method chosen for this section is therefore to compare the RTD sensor to closest thermocouple sensor, and compare the ultrasonic flowmeter to the closest thermocouple sensor, as to not introduce unnecessary heat losses, and in turn errors, to the analysis. The RTD sensor and ultrasonic flowmeter can in turn be compared with beckground in the comparison to the thermocouplers.

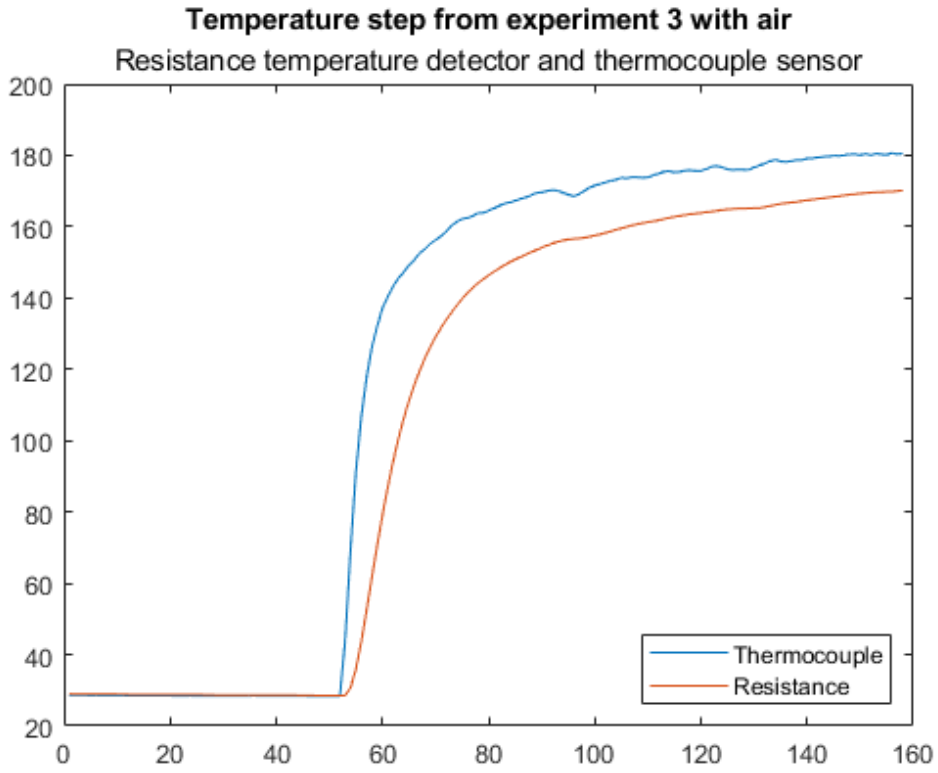


**Figure 7.5.:** Temperature step for thermocouple sensor compared to the RTD

In figures 7.5 and 7.6 the isolated step for the RTD & thermocouple close to the RTD, and the ultrasonic flowmeter & the thermocouple close to the ultrasonic sensor is presented respectively. As before in section 7.2.1 system identification will be performed on the data to extract both a delay and a pole location.

The results of the delay estimation was 1 sample (1 second using sample frequency 1 Hz), except for the RTD which had a dead-time of 2 samples (2 seconds respectively). The result reflects quite low to no delays, but it is notable that the RTD has a slightly longer dead-time, up to two seconds.

The estimated transfer functions resulted in the following: the RTD transfer function had pole in -0.07753 with 96 % fit, the thermocouple close to the RTD transfer function had pole in -0.1867 with 91.95 % fit, the ultrasonic flowmeter transfer function had pole in -0.07335 with 83 % fit, and the thermocouple close to the ultrasonic sensor transfer function had pole in -0.0957 with 85 % fit.

From the transfer function estimations the general speed of the sensors can be determined.

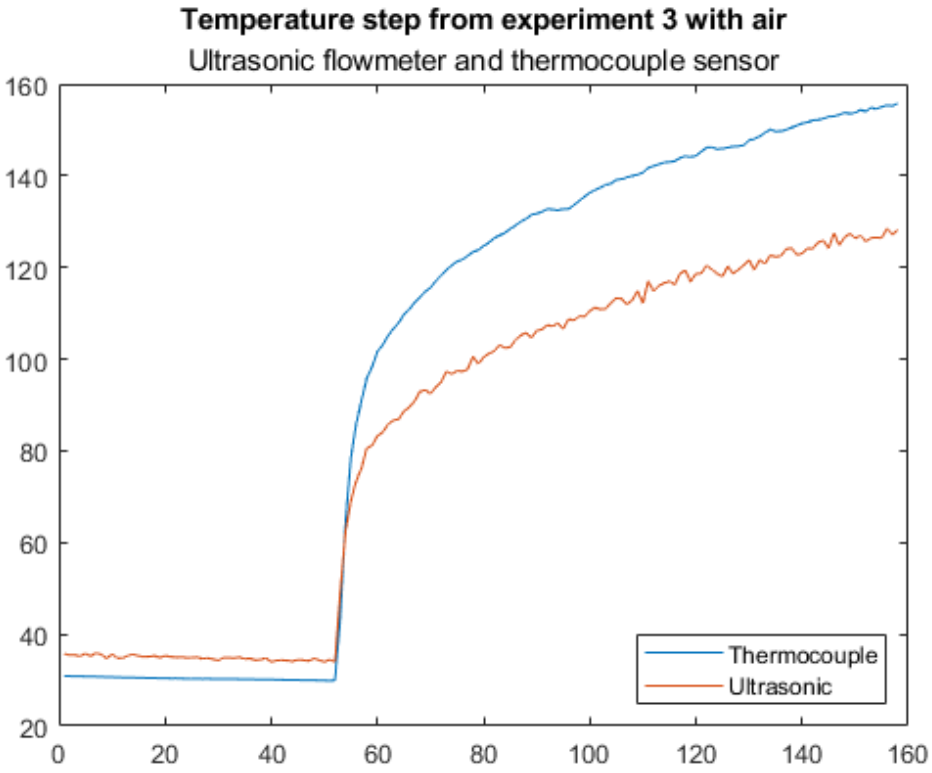


**Figure 7.6.:** Temperature step for thermocouple sensor compared to the ultrasonic flowmeter

The RTD is notably slower that the thermocouple sensor, but the ultrasonic flowmeter is only slightly slower than the thermocouple sensor, implying measuring the speed of sound is a viable alternative to traditional temperature sensors. It does also reflect poorly on restistance temperature detectors as it was the relatively slowest sensor of the compared sensor types.

The analysis of sensor speed may be of interest, but it must also be mentioned that no account for the accuracy of any of the sensors were taken, as the actual air temperature during the experiments could not be measured. One can observe a stationary, or growing, error between the compared sensors in the step plot, this is not accounted for but noteworthy as a stationary error could be interpreted as one of the sensors being more accurate than another. It is, for example, likely that the parameters is not entirely accurate when calculating the temperature of the medium based on the measured sound of speed, giving way for the large discrepancy.

The final experiment, experiment 4, could be used for accuracy estimation of the sensors, in theory, as the electric heater is controlled to a given temperature. The idea is flawed, however, as the heater is controlled using a thermocouple sensor, giving the thermocouple

sensor type a clear advantage of being the type of sensor controlled for. Furthermore, the discussion of losses could still be applicable for this experiment, and the location of the sensors would yet again come into play.

# Chapter 8.

# Conclusions

## 8.1. Models

Over the experiments conducted on ETHEL, an average relative error of 10 % was found. As the model construction of ETHEL was similar to that of the model of system 1010 the assumption of a similar relative error in the system 1010 model is not unreasonable, which is quite a large error in reference to the high temperatures that system 1010 use.

In the model of ETHEL, the conclusion can be drawn that unmodeled features may have led to unexpected behaviours and errors. The point is not directly transferable to system 1010, since the system 1010 model does include models of the pressure control system and leaks. The point is broadly applicable, though, and consideration of the system delimitations in section 3.1.1 should be made. In a complex system, made up of many interconnecting systems, it is not always obvious which variable is affecting which outcome.

The results gained from ETHEL and the ETHEL model may have errors caused by the amount of air in the system during helium only experiments. The estimation of air showed upon 5 - 15 % air in any given experiment with helium, though the model used only helium as medium. This would bode well for system 1010, which presumable will be using close to 100% helium.

The cross-correlation analysis and Pearsons correlation coefficient, however, implied a strong correlation between the model and the real data, meaning that the time-response behaviour of the model is fair for that of the real system.

Ways to improve further upon the model, and any model of the same type, would be to take the suspected error-inducing factors in regard, as previously described. This includes to further study the physical system to avoid unmodeled features, and to reduce the need for physical parameter estimations. As well as increasing complexity of the

model, knowing that doing so may reduce the user-friendliness of the model, and increase computation times.

## 8.2. Sensors

The model of ETHEL contains many similarities to the system 1010 model in function and construction, and beyond that, its behaviours in the experiments could be likened to the ETHEL behaviours. With that conclusion as a background, one can extrapolate the conclusions made about ETHEL and the model, to, system 1010 and the system 1010 model. One being that the time response of the model is similar to that of the real system. It is therefore fair to assume that any time-response analysis conducted on the system 1010 model is accurate for system 1010.

The system identification showed that the dead-time behaviour of the temperatures in system 1010 was not significantly affected by their location in the cooling loop, i.e. the length of piping between the sensor point, and the target wheel. However, it did affect the speed of convergence for the measured temperatures somewhat. The result implies that the delay originates from the target wheel, and the issue of delay in the sensors is not easily solvable by relocating the sensors.

Temperature sensors of different types were evaluated, in particular the speed of the sensor types relative to each other was estimated. In order from fastest to slowest the results were: thermocouple sensor, ultrasonic flowmeter, and resistance thermal detector. The result is surprising, as the ultrasonic flowmeter would not need to absorb heat to measure it, but the discrepancy may be explained by losses between the relevant sensors as seen in figure 3.5. Furthermore, it may also be impacted by the large mass of the ultrasonic flowmeter build, it may have absorbed heat and lead to cooler medium within and after the flowmeter. Lastly it can be observed that the RTD sensor is the slowest by a far margin, however the delay detected in the sensor is still only on the range of a few seconds, and in the system 1010 cooling loop the few seconds has a minuscule impact on the normal 40 second dead-time detected in the location analysis.

## 8.3. Reflection and future work

With the background in the analysis and results from ETHEL and the ETHEL model, it is fair to say that the system 1010 model is qualitatively accurate, though not quantitatively accurate, for the real system 1010. And any result of the model must be viewed with

some scepticism.

Furthermore, the system 1010 temperatures are slow, which is not so much caused by the piping, nor losses through the insulation, but rather by the energy absorbed by the massive target wheel. Thus the temperature measurements taken outside the target wheel should also be viewed with care.

This project is limited in its scope, only looking at some properties of the sensors, only evaluating models in a few ways. The project is at the same time quite diverse, as it tackles issues from physical modelling, down to the minutia of the fluid dynamics, to model evaluation using statistical methods. Suggestions for future work could therefore be to dig down deeper in any of these topics, for example how to in an empirical sense test and evaluate the quality of models, or how to construct good faithful models of cooling systems of this type. Another suggestion could be to have a broader perspective, less based on a single case and instead looking at generalities when it comes to the work processes described in this project.

# Bibliography


[1] *European spallation source*, https://europeanspallationsource.se/about, Online; accessed: 2022-02-07.

[2] *ESS revises project plan and budget*, https://europeanspallationsource.se/article/2021/12/10/ess-revises-project-plan-and-budget, Online; accessed: 2022-05-24.

[3] *Pandemic causes ESS to adjust project plans*, https://europeanspallationsource.se/article/2021/03/25/pandemic-causes-ess-adjust-project-plans, Online; accessed: 2022-02-07.

[4] *ESS organisation*, https://europeanspallationsource.se/ess-organisation, Online; accessed: 2022-02-09.

[5] *Construction of the ESS buildings and landscape is completed*, https://europeanspallationsource.se/article/2021/12/22/construction-ess-buildings-and-landscape-completed, Online; accessed: 2022-02-07.

[6] *Science using neutrons*, https://europeanspallationsource.se/science-using-neutrons, Online; accessed: 2022-02-09.

[7] *Neutrons: The science of everyday life*, https://europeanspallationsource.se/ess-mandate/neutrons-science-everyday-life, Online; accessed: 2022-03-15.

[8] *Chemistry of materials, magnetic & electronic phenomena*, https://europeanspallationsource.se/science-using-neutrons/chemistry-materials-magnetic-electronic-phenomena, Online; accessed: 2022-03-15.

[9] *System definition - solution target helium systems*, Internal document ESS-0012527; revision 6.

[10] *Qualitative radiological hazard analysis - target systems (1000) and target helium cooling systems (1010, 1011, 1013)*, Internal document ESS-0037525; revision 4.

[11] T. Glad and L. Ljung, *Reglerteori Flervariabla och olinjära metoder*, 2:9. Studentlitteratur, 2017.

[12] *Modelica language*, https://modelica.org/modelicalanguage.html, Online; accessed: 2022-03-01.

[13] *Verification of modelica target helium cooling 1010*, Internal document ESS-3416837; revision 1.

[14] K. J. Keesman, *System Identification: An introduction*, 1st ed. Springer, 2011.

[15] *Modelica language*, https://modelica.org/modelicalanguage.html, Online; accessed: 2022-05-20.

[16] *ModelicaStandardLibrary*, https://github.com/modelica/ModelicaStandardLibrary, Online; accessed: 2022-05-20.

[17] *The modelica fluid and media library for modeling of incompressible and compressible thermo-fluid pipe networks*, https://modelica.org/events/modelica2006/Proceedings/sessions/Session6b1.pdf, Online; accessed: 2022-05-20.

[18] P. Dermont, D. Limperich, J. Windahl, K. Prölss and C. Kübler, *Advances of zero flow simulation of air conditioning systems using Modelica*, https://ep.liu.se/ecp/124/018/ecp16124018.pdf, Online; accessed: 2022-05-03.

[19] *Compare - description*, https://se.mathworks.com/help/ident/ref/compare.html#description, Online; accessed: 2022-05-25.

[20] *How to normalize the RMSE*, https://www.marinedatascience.co/blog/2019/01/07/normalizing-the-rmse/, Online; accessed: 2022-05-25.

[21] *goodnessOfFit*, https://se.mathworks.com/help/ident/ref/goodnessoffit.html, Online; accessed: 2022-05-25.

[22] *Relative error: Definition, formula, examples*, https://www.statisticshowto.com/relative-error/, Online; accessed: 2022-05-25.

[23] T. R. Derrick and J. M. Thomas, *Time series analysis: The cross-correlation function*, https://www.statisticshowto.com/relative-error/, Online; accessed: 2022-05-26, 2004.

[24] M. Saeed, *Calculating pearson correlation coefficient in python with numpy*, https://stackabuse.com/calculating-pearson-correlation-coefficient-in-python-with-numpy/, Online; accessed: 2022-05-26.

[25] *Altosonic v12*, https://www.manualsdir.com/manuals/369187/krohne-altosonic-v12-en.html, Online; accessed: 2022-05-20.

[26] W. Moebs, S. J. Ling and J. Sanny, *University physics: Volume 1*, Open source textbook; last updated Feb 10, 2022, 2016.

[27] P. A. Tipler and G. Mosca, *Physics for Scientists and Engineers*, 6th ed. W. H. Freeman and Company, 2008.

[28] *Steady heat conduction*, https://www.sfu.ca/~mbahrami/ENSC%20388/Notes/Staedy%20Conduction%20Heat%20Transfer.pdf, Online; accessed: 2022-05-20.

[29] R. H. S. Winterton, *Where did the dittus and boelter equation come from?*, http://herve.lemonnier.sci.free.fr/TPF/NE/Winterton.pdf, Online; accessed: 2022-05-24, 1998.

[30] *Fluids – lecture 6 notes*, https://web.mit.edu/16.unified/www/FALL/fluids/Lectures/f06.pdf, Online; accessed: 2022-05-24.

[31] *Thermal conductivity of gases chart*, https://www.engineersedge.com/heat_transfer/thermal-conductivity-gases.htm, Online; accessed: 2022-05-09.

[32] *Comparing the thermal conductivity of stainless steel to other metals*, https://www.stainless-structurals.com/blog/comparing-the-thermal-conductivity-of-stainless-steel-to-other-metals/, Online; accessed: 2022-05-09.

[33] *Gases - dynamic viscosities*, https://www.engineeringtoolbox.com/gases-absolute-dynamic-viscosity-d_1888.html, Online; accessed: 2022-05-09.

[34] *Gases - specific heats and individual gas constants*, https://www.engineeringtoolbox.com/specific-heat-capacity-gases-d_159.html, Online; accessed: 2022-05-30.

[35] *Delayest - description*, https://se.mathworks.com/help/ident/ref/delayest.html#f4-1606208, Online; accessed: 2022-05-24.

[36] *Oe - more about*, https://se.mathworks.com/help/ident/ref/oe.html#mw_65e4d591-6e45-4cc1-bfda-db27136cb7da, Online; accessed: 2022-05-24.

[37] S. Sundaram, *Ece 380: Control systems*, https://engineering.purdue.edu/~sundara2/misc/ece380_notes.pdf, Online; accessed: 2022-05-24, 2014.

[38] *Maintenance of target cooling systems*, Internal document ESS-3628544; revision 1.

[39] *Target primary cooling P&I diagram*, Internal document ESS-0040854; revision 6.

[40] *SDD-Sol system 1027 - monolith rough vacuum pump system*, Internal document ESS-0134942; revision 2.

[41] *Technical specification system 1015 - helium purification system*, Internal document ESS-0069152; revision 2.

[42] *Instruction manual for the operation and maintenance of the helium cooling circulators*, Internal document ESS-0105209B; revision 2.

[43] *Project: ESS helium circulator ref 17SMN013: WP1 report aerodynamic wheel and venturi flowmeter design by CFD*, Internal document ESS-0105206; revision 1.

[44] *Review comments for verification of modelica HX for 1010 and 1046 (ESS-3278982.1 VERSION 5)*, Internal document ESS-3278982; revision 1.

[45] *Computational and experimental investigation of cooling flow in a low Reynolds number pressurized helium loop*, Internal document ESS-0508017; revision 1.

[46] J. Klingmann, *Measurements 180524*, Not published; on behalf of ESS.

[47] *Draft CFD of ETHEL speed of sound*, Internal document ESS-2772342; revision 1.

# Appendix A.

# Images of ETHEL

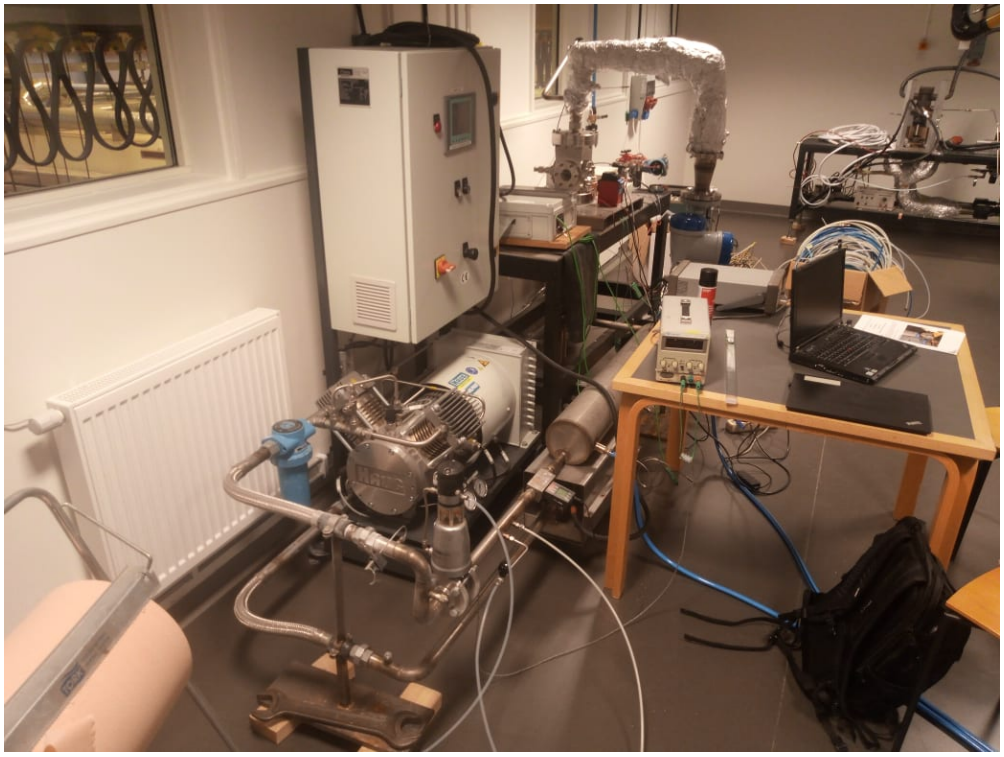


HAUG
OILFREE

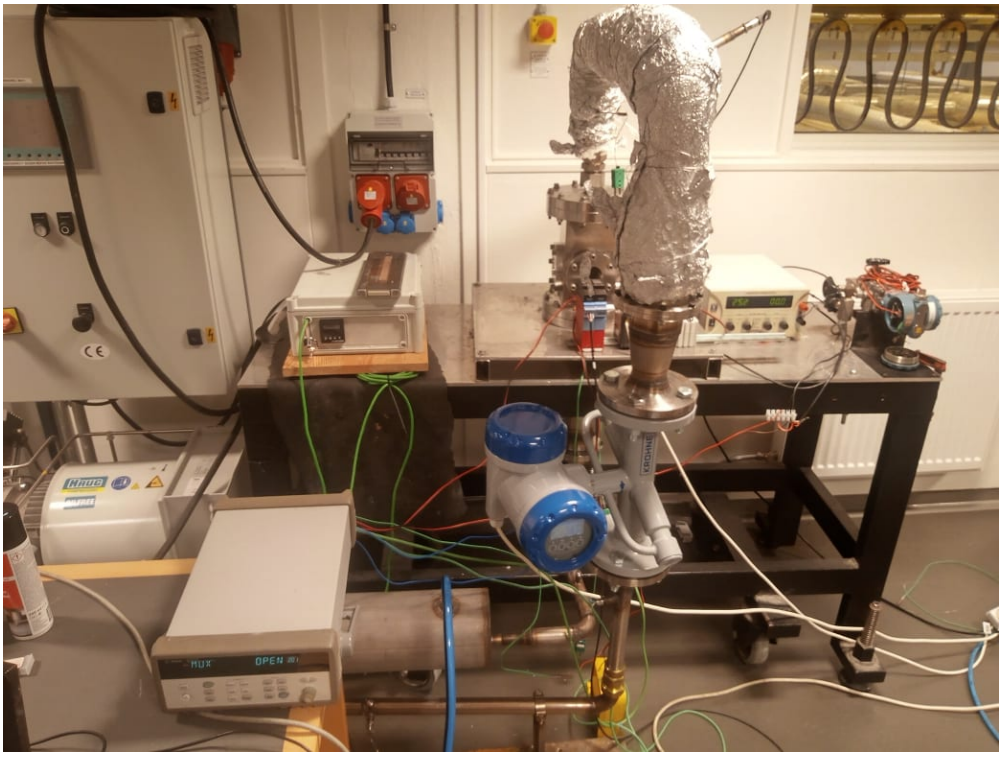
MUX
OPEN

# Appendix B.

# Matlab code used for system identification

```
tempstep = importdata("C:/data/path.mat");

t = table2array( tempstep(:, 1) );

u = table2array( tempstep(:, 2) );

y_wheel = table2array( tempstep(:, 5) );
y_sens = table2array( tempstep(:, 4) );
y_prefilter = table2array( tempstep(:, 3) );

t_index = diff(t) >= 0.5;

t_clean = t(t_index);
y_w_clean = y_wheel(t_index);
y_s_clean = y_sens(t_index);
y_p_clean = y_prefilter(t_index);
u_clean = u(t_index);

data_wheel = iddata(y_w_clean, u_clean, 0.5);
data_sens = iddata(y_s_clean, u_clean, 0.5);
data_prefilter = iddata(y_p_clean, u_clean, 0.5);

delay_wheel = delayest(data_wheel);
delay_sens = delayest(data_sens);
delay_prefilter = delayest(data_prefilter);

tf_wheel = tfest(data_wheel, 1, 0, delay_wheel, 'Ts', 0.5);
tf_sens = tfest(data_sens, 1, 0, delay_sens, 'Ts', 0.5);
tf_prefilter = tfest(data_prefilter, 1, 0, delay_prefilter, 'Ts', 0.5);
```